

HyparActive

A Design Exploration Tool for Multi-segment Hyperbolic Paraboloid Shells

Winston Davis

A thesis submitted in partial fulfillment of the requirements for the degree of:

Master of Science in Architecture

University of Washington

2016

Advising Committee:

Brian R. Johnson

Tyler Sprague

Program authorized to offer degree:

Department of Architecture

© Copyright 2016
Winston Davis

University of Washington

Abstract

HyparActive

A Design Exploration Tool for Multi-segment Hyperbolic Paraboloid Shells

Winston Davis

Chair of the Advising Committee:

Brian R. Johnson

Department of Architecture

While thin shell structures could offer efficient solutions to modern design problems, designer familiarity with the strengths and limitations of the form have declined in recent years. Thin shell structures are seeing a resurgence of interest due to modern fabrication techniques, but are hampered by the difficulty of balancing form manipulation and structural analysis concerns during early design. In this paper we describe HyparActive, a software tool developed specifically to help designers explore and design a remarkably wide range of thin shell forms. HyparActive provides simple interactive 3D form-manipulation tools for the designer and quick Finite Element Analysis (FEA) feedback regarding the shell's structural behavior. Developed in an algorithmic modeling environment, the tool allows users to define, manipulate and visualize a parametric form consisting of one or more hyperbolic paraboloid (hypar) shell fragments. The shell is put through a quick FEA analysis, using user-specified material properties, and the resulting stresses are used to color-code the model rendering, highlighting overstressed areas. The quick feedback available on a standard PC means the designer can interactively explore how form and stress distributions interact, informing design decisions and enhancing their design "intuition." The thesis also reflects on the challenges of developing an interactive learning tool in a parametric modeling environment and the benefits of including performance analysis in the conceptual design phase.

Acknowledgements

I would like to thank my advisory committee for their guidance and the DMG community for their encouragement during this exploration. I would not have been able to learn and accomplish so much without such a supportive environment and engaging faculty.

I would also like to thank my family and friends for their encouragement throughout this endeavor. It would not have been possible without your support.

Table of Contents

Historic Context	
Basic Thin Shell Forms	6
The Golden Era	8
Fall from Popularity	10
Contemporary and Future Thin Shells	
Technological Innovations	11
Digital Workflows	14
Case Studies	15
What is Delaying a Thin Shell Revival?	17
Why Should Designers Start Using Shells Again?	18
HyparActive	
Design for Learning	19
Shell Form Synthesis	20
Final Control Scheme	23
Structural Simulation	24
Transient Data Spikes	25
Conclusions	27
Opportunities	29
References	
Bibliography	30
Figure Sources	32
Appendices	
A HyparActive User Manual	33
B Mesh Sensitivity Test Data	41

Historic Context

Reinforced concrete has been used in thin shell construction for a little over a century, attracting architects and engineers with its economical long-span capabilities. The initial interest in shells, undoubtedly, was the economy of their span-to-thickness ratio, not uncommonly upwards of 400 to 1.¹ Thin shells' structural economy stems from the "membrane action" that shells use to carry loads. This state of stress consists of compression, tension, and shear stresses, but no bending stresses (such as those acting on beams) within the thickness of the shell. When configured correctly, relatively small stresses in shell construction can be resisted by a small thickness of material, allowing for large span possibilities to be achieved with only minimal thicknesses.^{2, 3}

Reinforced concrete was initially developed for horticultural troughs, giant flower pots for palm trees, but the technology quickly found its way into building construction. French engineer E. Freyssinet was an early adopter of the technique, using it to build a parabolic barrel vault with a 30-meter span for a factory in 1905.⁴ Freyssinet is also credited with designing the first conical shell, and often favored the more complex geometry over simple barrel vaults.⁵

The domes of Centennial Hall, designed by Max Burg in Germany in 1912, are some of the first modern applications of reinforced concrete domes.⁶ Burg's Centennial Hall was also the first shell whose span exceeded that of the Pantheon in Rome. The 1920's saw more complex geometry develop in thin shell use. Monolithic domes were broken down into n -sided "polygonal" domes, with the corresponding construction broken down into pouring two oppositely-oriented sections at a time. This allowed builders to reuse formwork, significantly cutting cost of construction. This

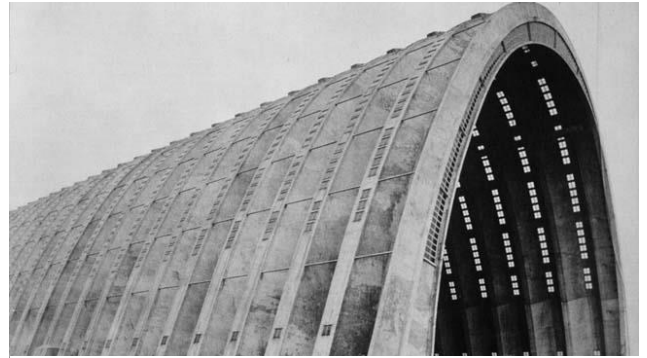


fig. 1 Dirigible Hanger by Freyssinet, built 1921

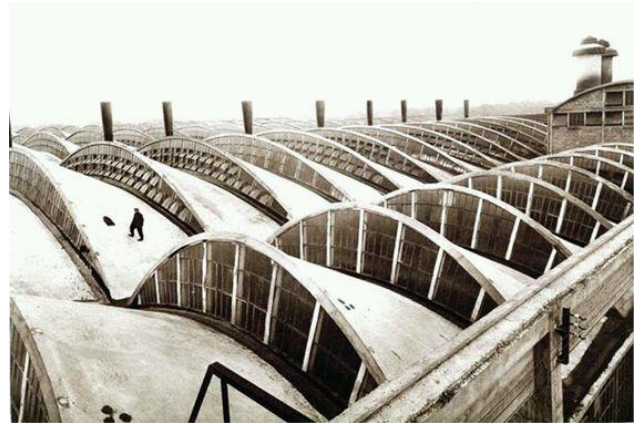


fig. 2 Conical shells by Freyssinet



fig. 3 Centennial Hall, built 1912

¹ Peerdeman et al. pg 1

² Bechthold pg 1

³ Peerdeman et al. pg 1

⁴ Krivoschapko et al. pg 1

⁵ Ibid. pg 2

⁶ Ibid. pg 3

strategy of component shells introduced a new paradigm for shell conception and execution.⁷

The basic geometry of these forms was key to their structural engineering success. An application of how the stresses in an arch are resisted and the addition of stiffeners and edge beams were the go-to strategy for making sure the shell was structural. This left little to change in the formal design. A few geometric attributes could vary, but the shapes were mostly prescribed. This out-dated design constraint is the source of the common misconception that thin-shell construction still requires a simple shape.



fig. 4 Leipzig Market Hall, built 1929



fig. 5 Stiffeners supporting shell, Hershey Arena built 1936

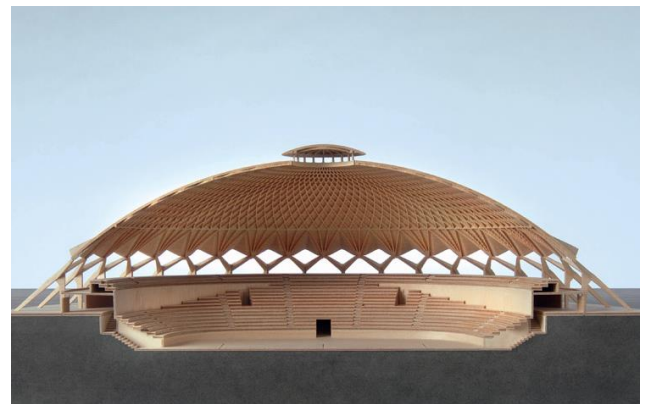


fig. 6 Model of Nervi's Palazzetto del Sporto, built 1957

⁷ Krivoschapko et al. pg 7

The Golden Era's Complex Forms

The period spanning the 1950's and 60's has been described as the "golden era" for thin shell construction. The boom in shell construction and development stemmed from the end of World War II: low labor costs caused by a surge in the number of people looking for work and the shortage of other construction materials, mainly steel.⁸ The economy of shells attracted designers and project owners alike, and their popularity triggered a period of rapid development in design and construction techniques. The development of more complex forms such as ellipsoid domes and hyperboloid surface structures were well-received by those less interested in basic domes and barrel vaults, but no form generated more interest in thin shells than the hyperbolic paraboloid, made famous by engineer Felix Candela.^{9 10}

The hypar form offers unique structural behaviors due to its anticlastic shape (having a positive curvature in one direction and negative in the other, bracing the form in two directions), and relatively simple constructability (due to it being ruled in both directions). Additionally, the form offers a high range of formal flexibility while retaining its structural behaviors and embedded construction logic.

Candela became known for his striking hypar forms which always appeared lighter and more graceful than traditional shell forms. Candela accomplished this through a masterful understanding of geometry. He used his knowledge of how the surface's geometric and material attributes would affect its resistance of structural stresses to design very efficient forms. He also integrated additional structure into the forms by thickening instead of using the traditional stiffener ribs and edge beams. In the case of Los Manantiales, he simply chose a form he knew would both render the compression and tension stresses negligible and sufficiently hide the thickened beams.¹¹

In contrast to Candela's geometric "purity of form" approach, some designers chose to conduct physical



fig. 7 Pavilion based on Candela's design



fig. 8 Auditorio Juan Pachín Vicéns in Ponce, Puerto Rico

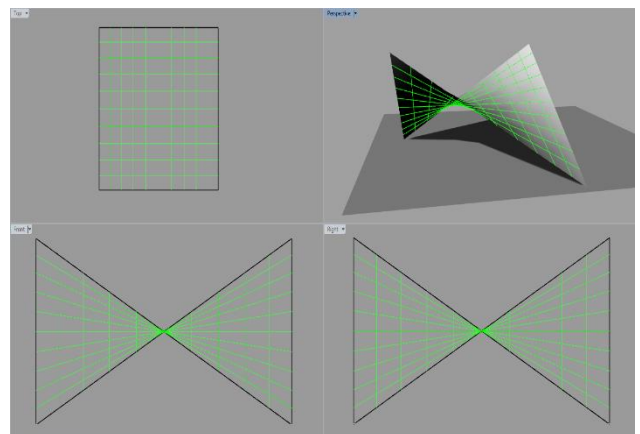


fig. 9 Linear isocurves of Hypar in Rhino 3D

⁸ Peerdeman et al. pg 2

⁹ Ibid. pg 7

¹⁰ Ibid. pg 17

¹¹ Burger et al. pg 3

experiments to discover funicular surface forms. The experimental forms of Swiss engineer Heinz Isler are some of the most creative and geometrically flexible thin concrete shells. At model scale, Isler used physical forces like gravity and air pressure to morph elastic materials, hanging models, soap bubbles, and expanding foam into stable funicular forms. Once a stable model was created, it was meticulously measured within a few hundredths of a millimeter to derive dimensions to scale up and use to produce formwork.¹²

While it certainly has produced elegant and efficient forms, Isler's method has some disadvantages. The process of finding best-fit forms inherently relinquishes the designer of much geometric control. This trade-off often produces a mostly-prescribed shape that is esthetically similar to many other funicular forms. Isler is said to have even been able to reuse formwork on multiple projects involving completely different shell designs.¹³

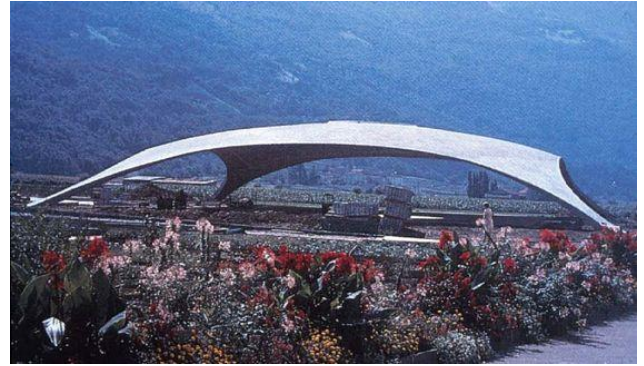


fig. 10 Bürgli Garden Center, Heinz Isler, built 1973



fig. 11 Deitingen Service Station, Heinz Isler, built 1968

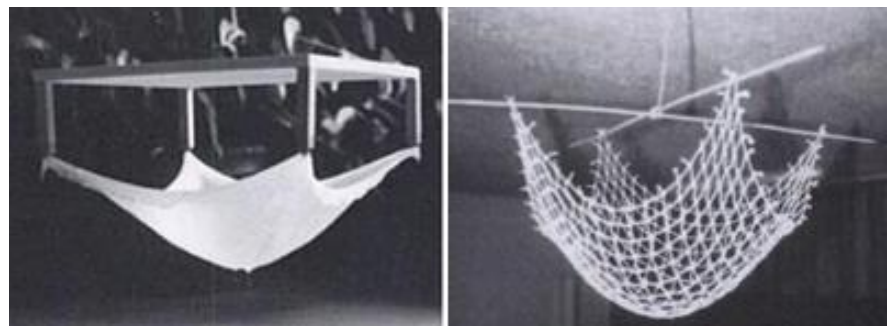


fig. 12 Physical form-finding through models

¹² Isler pg 1-2

¹³ Ibid. pg 5

Shells Fall from Popularity

The golden age of thin shells came to an end in the early 1970s. Brought on by a multitude of reasons, the production of thin concrete shells around the world dropped off abruptly. Construction costs are widely regarded as the main reason for the decline in shell use. Skilled labor costs increased by a factor of 11 in the fifty years following the shell boom of the 50's.¹⁴ Requiring a high percentage of skilled labor, construction costs for shells rose quickly.¹⁵ To make matters worse, energy codes for buildings were made much stricter by the oil crisis in 1973. While an efficient structural material, concrete has poor insulating abilities, and the cost of incorporating insulation into the traditional method of constructing shells was significant.¹⁶

These new cost challenges came at a time when other, cheaper material choices were becoming popular. The use of space frames, cable nets, and fabric structures offered solutions that provided economical spans as large as concrete, but whose constructional requirements were much more easily met.¹⁷ The use of skeletal grid shells, most commonly realized through the utilization of welded steel beams (at the time, a relatively new development in building construction), also cost less to construct.

These new construction strategies also offered designers more formal freedom than the strict symmetry enforced by most shell design methods of the time. This accelerated the shift of traditional shell forms from stylish to passe.¹⁸ Traditional thin shell design methods simply could not satisfy society's new desire for expressive "free form" architecture.

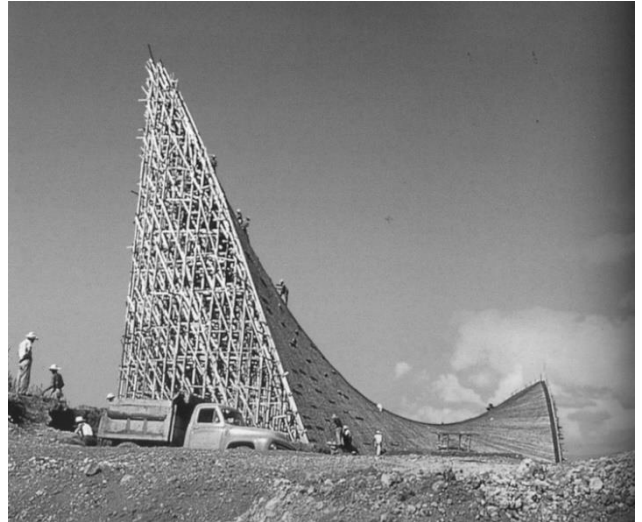


fig. 13 Construction of Candela's Chapel Lomas de Cuernavaca, 1958

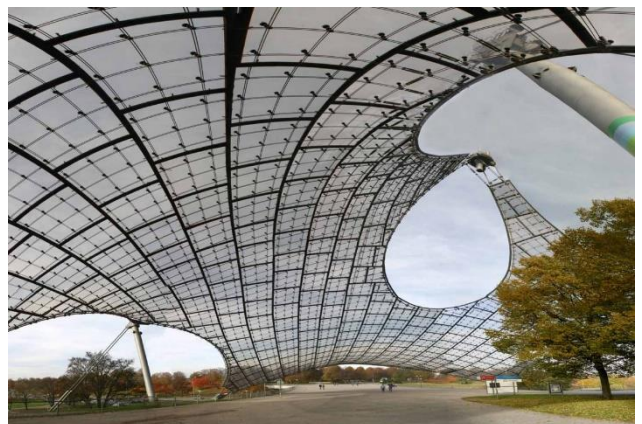


fig. 14 Munich Olympic Stadium, 1972

¹⁴ Bechthold pg 3

¹⁵ Meyers and Sheer pg 4

¹⁶ Weller pg 15

¹⁷ Bechthold pg 2

¹⁸ Meyers and Sheer pg 4

Contemporary and Future Thin Shells Innovations in Design Technology

Although shells fell out of popular standing, development of their design and construction processes has continued. One construction innovation is the use of inflatable formwork. Popularized by Dante Bini in the 70s and 80s, one of the most popular contemporary shell construction strategies still incorporates inflatable formwork.¹⁹ This *Monolithic* process, developed by David and Barry South, involves spraying foam onto an inflated form. The foam holds the weight of the reinforcing steel set in place and then the weight of the shotcrete that is applied in the final step.²⁰ Both the use of inflatable formwork and force-applied concrete has cut the cost of constructing these thin shells.

Another construction technique developed in the post-golden era is the practice of prefabrication. It was discovered that by precasting components with a reusable mold, and simply assembling the already-structural components on site, the economy of the thin shell was pushed even further by significantly reducing the costs of construction. Jack Christiansen, a structural engineer who has designed thin concrete shells for over 50 years, argues that prefabrication and modularity are key to the future development of thin concrete shells.^{21 22}

Technology has also affected how shells are conceptualized and designed. One obvious example is structural analysis through finite element models. Finite element analysis gives designers the ability to estimate how a design solution will perform through simulation. Analyses of historic structures give more detailed results than the original designers had access to, revealing interesting discrepancies; Torroja underestimated the stresses in his Fronton de Recoletos roof structure, but luckily made up for it with an edge beam added as a safety measure.²³ An analysis of Candela's Los Manantiales structure showed that he over-estimated the stresses created in the form, which were far under the

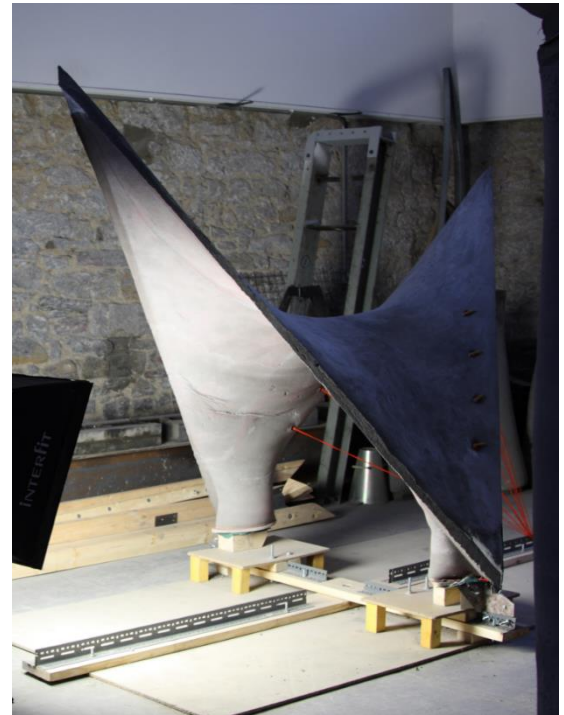


fig. 15 Prefabricated Hyper Component



fig. 16 Structural Simulation with Visual Feedback

¹⁹ Meyers and Sheer pg 4

²⁰ Ibid. page 4

²¹ Melaragno pg 192

²² Meyer and Sheer pg 6

²³ Lozano-Galant et al. pg 10

maximum allowable stresses for concrete.²⁴ This information being provided to designers earlier in the design process allows them to make better decisions and avoid problems that would be more difficult to fix later in the design process.

A more recent innovation, CNC fabrication equipment, has led to major developments in how shells can be subdivided, fabricated, shipped and assembled into even more efficient forms.²⁵ CNC mills have been used to fabricate adjustable frames that hold fabric liners to form many varieties of panels.^{26 27} CNC hotwire cutting has been utilized in the fabrication of foam molds. Due to the implicit nature of wire cutting, many varieties of ruled-surfaces can be made and used to cast concrete panels. One study has developed a process of making forms to cast doubly-curved panels that lock together like puzzle pieces when assembled.²⁸



fig. 17 Structure created with adjustable formwork

The 3D Printing boom of the past decade has made for interesting developments in the additive manufacturing of concrete as well. It isn't difficult to find examples of how 3D printing has affected the pouring process- what may matter even more is how it has affected the materiality of concrete. One study from Rael San Fratello Architects illustrates this through the creation of a high-strength concrete polymer. The design team developed a method of 3D printing fiber-reinforced concrete parts from a bed of concrete powder, affording much more complex shapes than traditional casting. The parts are then infiltrated with hardening agents that further strengthen the bonds in the concrete while hydrating it to also increase its strength. The result is a very strong concrete polymer that withstood stresses upwards of 4500 psi after only 14 days, twice the strength of traditional concrete given twice as long to cure. Other instances of "ultra-high performance concrete" have been produced and tested in construction. One prime example is a fiber-reinforced

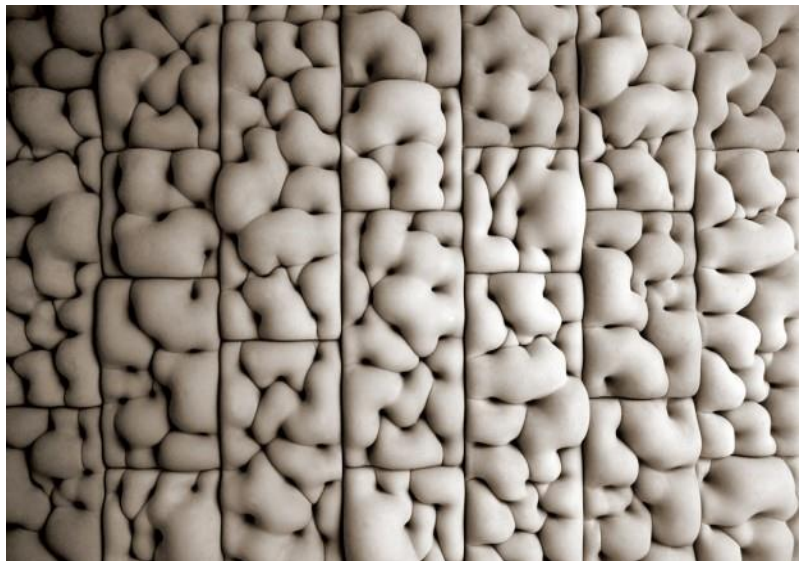


Fig. 18 Concrete forms created with adjustable formwork

²⁴ Garlock et al pg 148

²⁵ Bechthold pg 3

²⁶ Schwipper et al. pg 1

²⁷ Veendeeal et al. pg 6

²⁸ Martins et al. pg 4

shell built in Germany that covers 6900 square feet with a thickness of 10 millimeters.²⁹

Concrete isn't the only material being developed for use in shell construction. Many material experiments are being conducted to discover new methods of creating structural surfaces. One such experiment looks to one of the least structural materials one could consider: shrink wrap. The design team developed a method of subdividing a funicular shell form into a pattern of circles, which are fabricated from wood and fastened to a precision-cut piece of shrink film. The film is heated, causing it to contract and putting the circles in compression, causing the assembly to take the shape of the initial form.³⁰ There is much development needed for this technique to be considered for anything more than a pavilion, but the strategy certainly affords an impressive span to weight ratio.

Textiles are also being explored for use in structural surfaces. One study done at the Institute for Computational Design developed a method for robotically fabricating folded textile structures. The process involved simulating the folds in the fabric, and analyzing the placement and size of folds and creases for structural performance. Once a solution was reached, CNC robot arms folded the fabric into shape, which was then hardened by infused resin. While still more development is needed, the design team reports there is potential for incorporating many architectural requirements into the design of the folds, such as structural reinforcement, natural lighting, acoustics and thermal regulation.³¹



fig. 19 "Ultra-high performance", fiber-reinforced concrete



fig. 20 CNC-folded, structural fabric panel

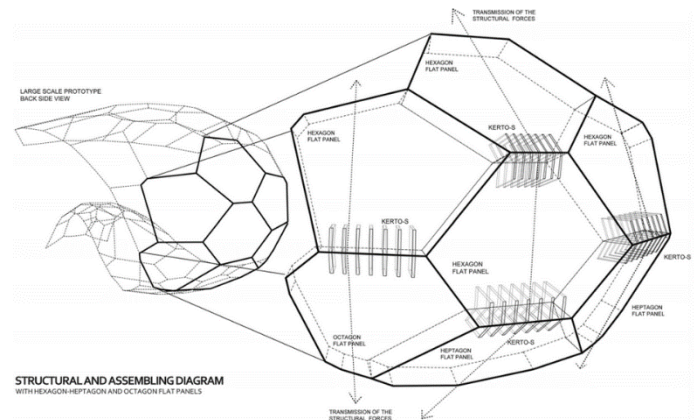


fig. 21 Joint detail for timber shell

²⁹ Meyers and Sheer pg 2

³⁰ Kuma pg 5

³¹ Kuma et al pg 7

Digital Workflows

The past decade's innovations in technology have had a profound effect on how shells are designed using computational methods. Parametric models allow for much more complex design solutions than traditional design methods by allowing designers to study more than one solution at a time. The potential afforded by finite element analysis grows exponentially when coupled with parametric modeling tools.

A study done at Harvard looked at a complex design strategy from the 1960's that integrated structural, natural lighting, drainage, and construction performance into static, repeated shell components. Once the geometric relations of the strategy were understood, they were applied to a complex doubly-curved surface.³² Without the use of parametric modeling, designing a form that performed under so many constraints would have been nearly impossible.

The coupling of complex geometry synthesis and automated performance analysis affords an unprecedented design environment. Instead of designing a complete object, and then testing its viability as a whole, designers are able to make changes and see the consequences almost immediately. This availability of information is necessary for what John Abel of Cornell said will be needed to bring shells back to popularity.³³ To make shells more economical, he says, a collaboration between design and construction teams will be necessary from the early design stages. The more intuition each team builds about the entire design and construction process, the more efficient and economical the project will be. Parametric modeling tools will certainly serve as a catalyst for this particular design movement and hopefully lead to more high-performance structures being built.

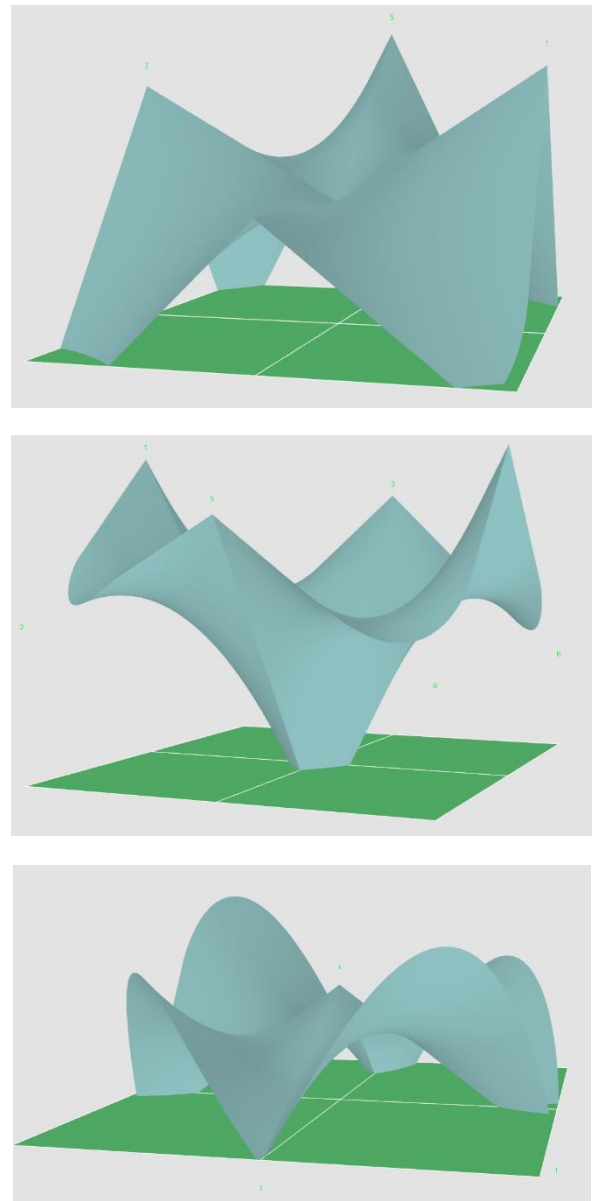


fig. 22 Various forms generated with one parametric model

³² Raspall et al. pg 6

³³ Meyer and Sheer pg 7

Case Studies: Digital Workflows for Producing Highly Efficient Shells

One research collaboration between design teams at the University of Michigan and the University of Technology Sydney illustrates how digital workflows can revive intriguing forms while cutting construction costs. The study set out to develop a method of subdividing a compressive shell form into planar panels that would then be used to generate self-supporting plates. The edge conditions of each plate were cut using abrasive water jets to be able to lock into the lower supporting row of plates in a way that would cantilever the plate. This method requires falsework for only a few panels; the rest are cantilevered when put in place, significantly lowering the cost of construction.³⁴

Two experimental projects done at the University of Stuttgart's Institute for Computational Design illustrate just how efficient computationally-deduced thin shell solutions can be. One experiment aimed to generate and fabricate a high-performance structural surface composed of woven fibers. The process involved modeling and analyzing a surface as if it were composed of the woven fibers and resin. Iterative generation and analysis helped find the most efficient arrangement of fibers in each panel. The form would then be made by weaving resin-impregnated-fiber onto a collapsible form by a CNC robotic arm. The fabrication of the form was also simulated in order to include that stage in the optimization process. The final product was a glass- and carbon-fiber shell pavilion that spans 8 meters with a thickness of 4 millimeters.³⁵

Another recent experiment was aimed at designing a timber-plate shell using an agent-based model and behavioral form finding. An agent-based model is used to define and simulate the interactions between various "agents". In this case, the agents were the wood panels generated from planar subdivisions of a doubly-curved shell form.



fig. 23 Monocoque carbon and glass fiber shell



fig. 24 Continuous fabrication of fiber shell

³⁴ Kaczynski et al. pg 1

³⁵ Reichert et al pg 11

Their attributes included shape, size, and position, structural and material composition, and toolpaths for fabrication; the interactions between them included structural stresses and finger jointing and other connection details. By being able to model the panels to that level of detail and simulate their behaviors, the design team was able to generate a high-performance solution: a 125 square-meter exhibition hall enclosed by an insulated and waterproof timber shell that spans 10 meters with 5 centimeters of material thickness.³⁶

These experimental structures are proof that digital design workflows are reviving intriguing, high-performance structures in the form of thin shells, while remaining highly economical in fabrication and construction.



fig. 25 Timber-panel shell exhibition hall

³⁶ Schwinn et al. pg 10

What is Delaying a Thin Shell Revival?

In 2005, a paper co-authored by Michael Sheer and Christian Meyer at Columbia University summarized the responses from many AEC professionals when asked about the general decline in interest in thin shells. The near-unanimous first answer as to why shells haven't experienced a comeback yet was cost. The second, by many of the respondents, was a reason relating to the freedom of form. Architects simply couldn't create the shapes they wanted with traditional shells. One respondent said that a common perception of thin concrete shells is that they are meant for economy-driven utilitarian projects and bulk storage, and lack the formal variety that contemporary signature structures are expected to have. An engineer at Arup went on to say that architects commonly feel constricted to a prescribed shape when considering shell construction and need more flexibility with form. One respondent reported this downside about the Monolithic process. They explained that the air-forms are often designed, manufactured and shipped without the input of an architect, leaving the final product aesthetically dull. Getting architects interested in designing shells again, they explained, is essential to increase their aesthetic appeal and bring them back into popularity.³⁷

Simply being unfamiliar with the forms is another factor constraining shell use today. A majority of the respondents to Meyers and Sheer believe that thin concrete shells are of little interest due to both the architects' unfamiliarity with structural systems they do not routinely use and their perceptions that shells won't fulfill their design requirements. One respondent hypothesized that a simple lack of information about shells is another reason for their lack of popularity.³⁸

³⁷ Meyers and Sheer pg 4

³⁸ Ibid. pg 4

Why Should Designers Start Using Shells Again?

Martin Bechthold explains in his essay *On Shells and Blobs* that a return to popularity by shells and structural surfaces is needed to create more efficient architecture and to break away from inefficiencies imposed by “blob” forms.³⁹ He explains that the curvature in blob forms, generated as they appeal to the eye, rarely allow membrane stress states to develop. These forms therefore depend on other structural systems that must absorb bending stresses, requiring much more material. Now that computational models allow designers to design with these aspects in mind, the designer needs to consider if they should take responsibility for creating an efficient structure, and at least consider a structural surface or shell form to see if it satisfies their design problem.

The problem is, current designers might not consider a shell for any number of reasons. Many architecture schools taught classes on designing shell forms when the practice was popular. Since then, the formal instruction on structural surfaces has fallen off, and today very few architecture schools offer the courses. Another obstacle is that shells are not routine for a majority of practicing architects, and when built, they are constructed using traditional methods.⁴⁰ Before architects will be willing to consider shells for contemporary projects, they must be familiarized with what contemporary shell technology can do for them. The problem is that the new digital workflows for designing complex shells is front-loaded with complicated programming. This intimidates and deters many architects, who traditionally have minimal computer-programming education. This apparent lack of information and design knowledge brought about the idea to develop a learning tool that helps users explore thin shell forms and understand how they work.

³⁹ Bechthold pg 1,2

⁴⁰ Peerdeman et al. pg 32

HyparActive

Design for Learning

The tool was designed in Grasshopper 3D, a parametric modeling plugin in for Rhinoceros 3D. Some important aspects of the learning tool have been identified to maximize the usefulness of the tool. The more complex aspects of the algorithm should be completely hidden, at least at first. This is important to not overwhelm the user by making available highly-complicated steps in the process they do not need to worry about. A strategy for accomplishing this in Grasshopper is compartmentalizing the definition using *clusters* and allowing the user to systematically dive deeper as they feel comfortable.

The tool should offer simple inputs and easy controls for changing variables, such as shape and material. It is important for the designer to be able to create interesting forms with a high level of control and flexibility. On the same note, the tool will need to communicate performance feedback in an easily-understood format, so the designers fully understand the consequences of their design decisions. Just as important as knowing exactly what is being changed is knowing that change's consequences.

Early in conceptual development, the decision was made to generate hypar shell forms. The hypar shows the most promise geometrically by affording a wide range of shapes with minimal parameters while maintaining its anticlastic form, and therefore its unique structural behaviors. Peerdeman offers a concise summary of why hypars are desirable forms for shells: "The success of the form rests for the architect in its appealing [geometry], for the structural engineer in its simple structural analysis, and for the contractor in its economical formwork".⁴¹

The goal was to develop a scheme for easily controlling a number of hypars to create a wide range of forms that would be constantly analyzed for structural viability and then to communicate this performance data visually through the same model.

⁴¹ Peerdeman et al. pg 18

Explorations in Shell Form Synthesis

The first exercise in generating hyperbolic paraboloid forms was to “project” a quadrilateral “onto” a hyperbolic paraboloid. The process involves extracting a grid of points from the initial quad surface, and calculating new Z coordinates (heights) for each point by using their X and Y coordinates as parameters for the hyperbolic formula. This produces a new grid of points that is used to generate a best-fit surface in the form of a trimmed hyperbolic paraboloid.

Using this algorithm, the hyperbolic geometry can be controlled with 6 parameters. This control scheme maximizes the range of forms available to the user by letting them control every attribute of the hyperbolic. The user can individually change the degree of curvature in each direction of the hyperbolic (see fig 27), as well as the “rotation” of the curvature relative to the quad (see figs 28, 29). Coupled with the capacity to shift the “balance” of the quad to one side of the hyperbolic (see fig. 30), a wide range of asymmetrical geometries can be achieved.

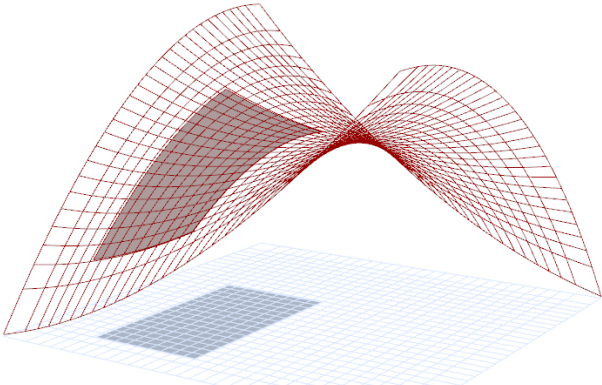


fig. 26 Flat quad projected to hyper above

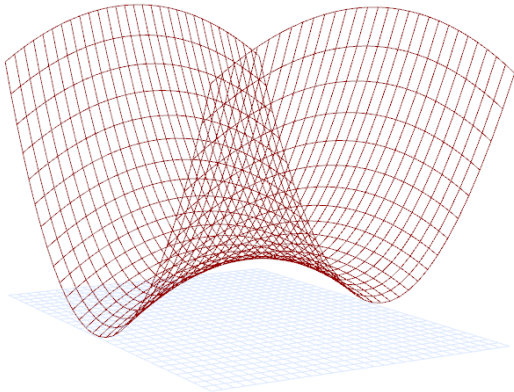


fig. 27 Projected hyper

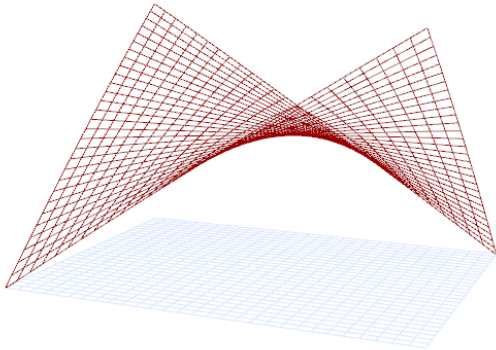


fig. 28 Projected hyper

Some disadvantages to the six-parameter control scheme were observed. Some redundancy in control was introduced by controlling both the height parameter and the c -variable parameter (from the hypar formula), which also affects the height. Using two parameters that affect the same attribute of the model causes some complication in achieving a desired form. Unfortunately, the c variable is not sufficient control of height without the other parameter. A second drawback is the level of abstraction between design intent and action. Even design constraints simple in conception proved challenging to realize with this control scheme. Simply keeping a specific corner in contact with the base plane became an exercise in data management. These hindrances abstract the design intent and can deceive the user, who either might not be making the changes they believe they are, or cannot figure out how to make the changes they want. While not particularly bad for the exploration of conceptual geometry, more parametric transparency is desired when designing built structures with specific formal requirements. When generating multiple hypars, each requiring six, individually-controlled input values, the control scheme became very cumbersome.

While developing an algorithm for generating a multi-segment hypar form, the control scheme was simplified. A single polygon was used to generate sets of four points, which were then used as parameters for Rhino's *Surface from Four Corner Points* command. The resulting surfaces were validated as hypars by checking their isocurves for linearity. This exercise provided some useful insight into generating hypars in Rhino's environment: the parameters could be simplified down to four points. This method of generating four points and creating a surface between them is much simpler than the projection method, however some loss of geometric control is observed: this method lacks the rotation and balance control afforded by the projection method and always generates a standard, untrimmed hypar.

This method of generating a radial composition introduced a useful constraint for further explorations: matching the edges of adjacent hypars. Making this constraint implicit within the algorithm certainly aids in the process of designing cohesive thin shell forms. It was later found that a single input form also improves the quality of the structural simulation.

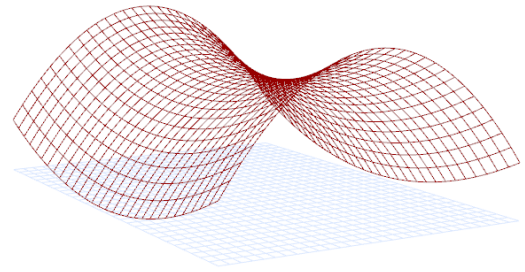


fig. 29 Projected hypar

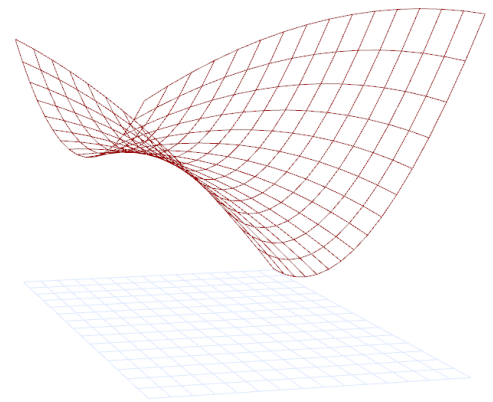


fig. 30 Projected hypar

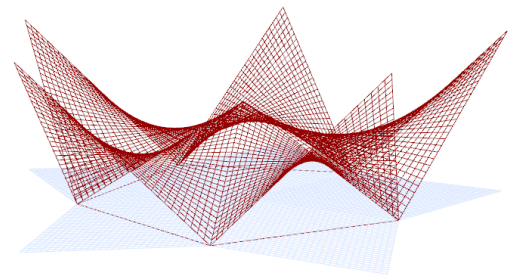


fig. 31 Radial configuration of hypar segments

The polygon used to generate the hypar forms evolved into a “footprint mesh”. This mesh is configured to be the flat footprint of the shell form. The user picks the size, configuration and number of segments to generate, and the corner points of each 4-sided segment are used to generate a hypar section. A grid configuration was developed to complement the radial configuration to give the user more form options.

The simplicity of these footprint configurations is a product of keeping the control scheme simple. Some explorations into allowing for more freedom in footprint configuration produces interesting results, but convoluted the interface with excessive parameters. Also, when using the four-point method of generating the hypars, the footprint mesh needs to be comprised of four-sided segments. If a robust control scheme could be developed that allowed for generation of trimmed hypars, i.e. using the projection method, it would allow for a less-constrained footprint mesh and allow for more complex subdivisions of the site.

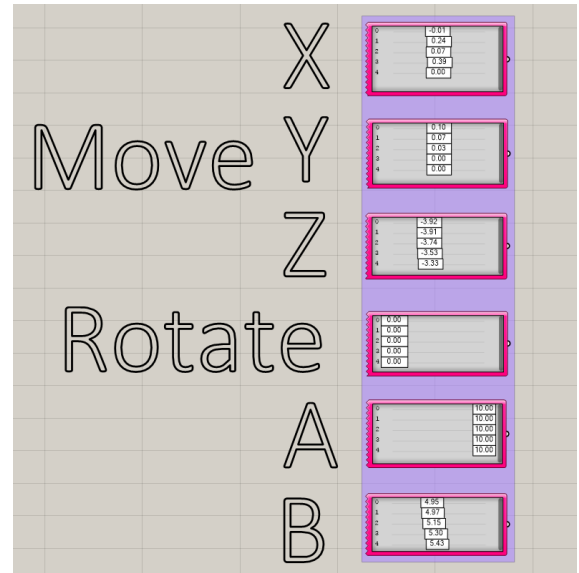


Fig. 32 Gene pool components providing five values for each parameter of five hypar segments

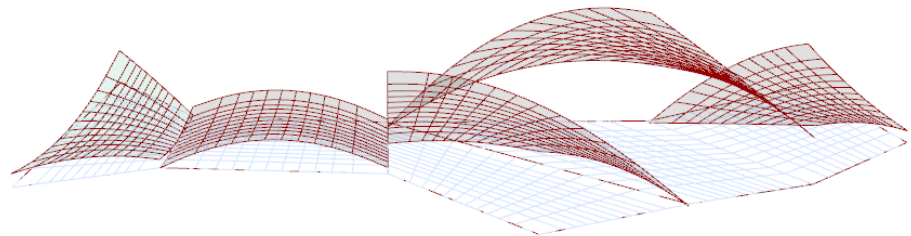


fig. 33 Five independently-generated hypar segments

Final Control Scheme

Compromises were made to simplify the control scheme that limited formal flexibility. This was necessary to allow the user to design multi-segment forms with a manageable control scheme. Finding the right balance between the level of control and simplicity of the control scheme illustrates the trouble of trying to design a learning and design tool with a focus on both. From an architectural design standpoint, the control scheme leaves more formal flexibility to be desired. However, the simple scheme serves the purpose of the learning tool and still allows the user to explore a wide range of asymmetrical forms.

Some quirks still exist as a result of translating something as simple as a point's Z-coordinate to something as complex as a concrete thin shell structure. To account for this, a user manual has been developed to introduce the control scheme and explain nonintuitive geometric relationships.⁴²

One opportunity that would greatly improve the user experience would be affording direct manipulation of the form and eliminating a large part of the separate control scheme all together. This would improve the level of control and interaction the user has with the form, while cleaning up the control scheme and resulting in a much less complicated user interface. More opportunities reside in the generation of the hypars. Developing a scheme of controlling hypars that meet on curved edges and being able to control that curvature would greatly increase the range of forms to be explored.

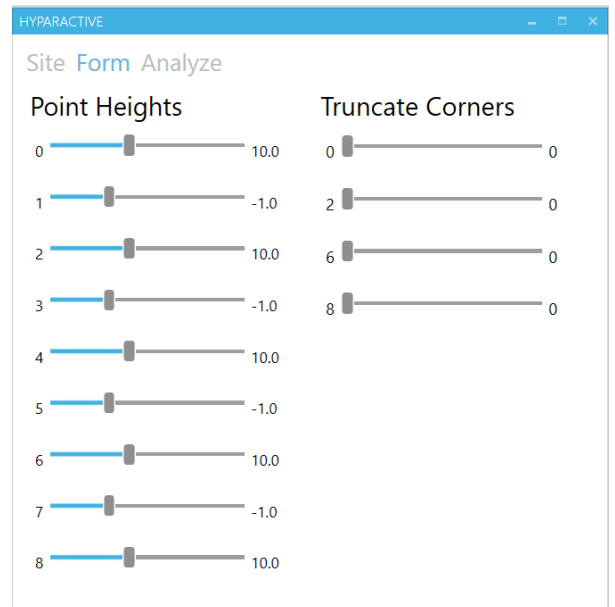


fig. 34 Final control scheme layout

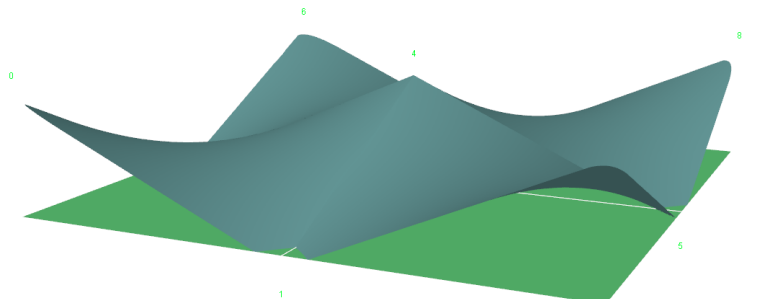
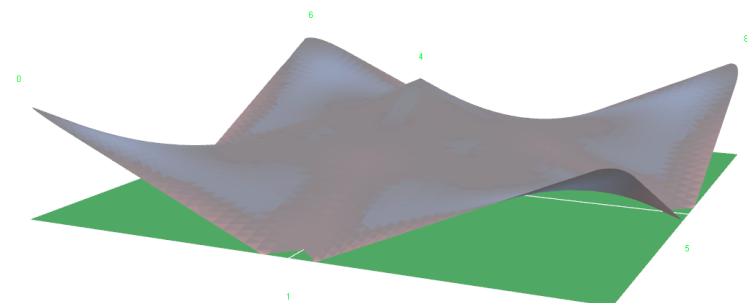


fig. 35 Model view: Blue shell form, green footprint mesh



Max Tension 137 psi
Max Compression 610 psi

fig. 36 Model view: Shell form colored by analysis feedback

⁴² See Appendix A

Structural Simulation

Providing the structural simulation functionality, Karamba, an FEA plug-in for Grasshopper, was used to analyze the form. The shell geometry is first converted to the format Karamba requires and in the process is subdivided into smaller elements. The density of these elements controls the precision of the analysis, so the value is parameterized so that a quasi-optimized value can be found. This value, referred to as the “mesh sensitivity” value, controls the relationship between the speed and the accuracy of the analysis, and since both are valued, a balance is necessary.

Three different forms were used to find an appropriate sensitivity value. The forms were analyzed using a range of sensitivity values starting at 0 and increasing by 50. The five highest values of each principal stress were recorded to identify an asymptotic curve that would provide a benchmark value to gauge the accuracy of the individual sensitivity settings. The time it took to calculate the solution was also measured for each iteration to help identify the most useful range. After comparing the results of all three forms, a value range of 500 to 700 was judged to provide the best balance of accuracy and speed.⁴³ Interestingly, the hypothesis that more elements always meant better simulation accuracy was not found to be entirely true. While the accuracy did increase overall, the frequency of eccentric results also increased, not to mention exponential increases in time requirements, which had to be considered in this experiment.

Some validation models were used to make sure the analysis tool was configured properly. Two forms of Felix Candela’s design were chosen to analyze as a similar analysis results from a study at Princeton were available for comparison. The analysis returned the largest principal tension and compressive stresses in each form, affording a total of four values to compare. The resulting sets of values are proportional and considerably close which provides a level of validity to the analysis of the tool.

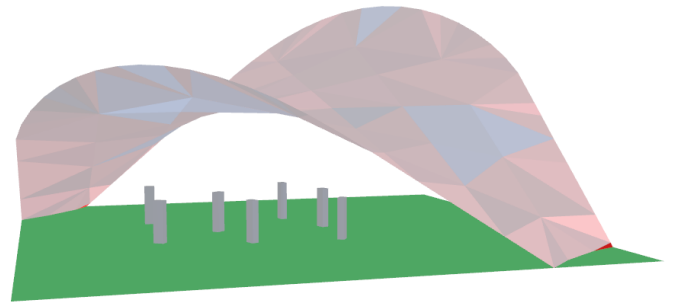


fig. 37 Mesh with low sensitivity value, individual elements easily distinguished

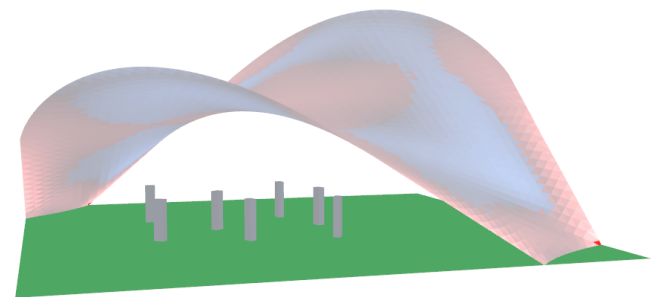
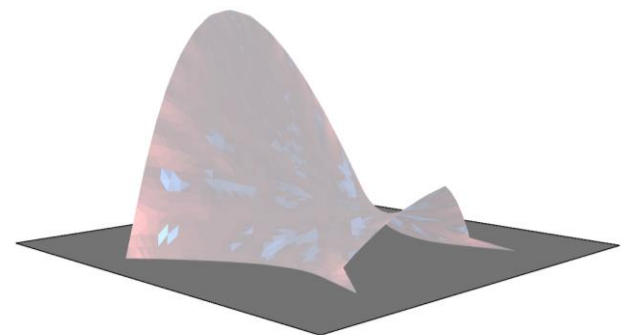


fig. 38 Mesh with high sensitivity value



Max Tension 177 psi
Max Compression 685 psi

fig. 39 Validation model

⁴³ See Appendix B

Transient Data Spikes

Some data spikes are seen in the stress values when compared to mesh sensitivity. While localized, the value spikes are unpredictable and could possibly blur the users understanding of the form's structural behavior. While investigating the cause of the spikes, it was observed that when a far-outlying value was returned, the surface area of the element producing that value was far smaller than the average element size. In one instance, the average element size was .85 square feet and the element responsible for the outlying value was .0003 square feet. It was also observed that these "problem elements" were consistently positioned at the bottom of the form, supporting the theory that the current method of trimming the form mesh with the ground plane is producing miniscule elements that produce highly inaccurate values.

Different solutions for this issue range from simply sensing that if problem elements exist in the model to preventing them altogether. Currently, the user is made aware if any problem elements currently exist in the model. The sham stress values provided by these elements are culled from the list of values displayed on screen. These elements are also rendered differently in the viewport to make the user aware of their presence and location in the model. At this point, the user is advised to try locally altering the form where the problem element is located. Minor adjustments are usually all that is needed to return a more uniformly-subdivided mesh after splitting it with the ground plane. This temporary solution consistently solves the value spikes while a system to prevent them is developed.⁴⁴

There are many opportunities for improving the effectiveness of the structural simulation. As observed, a workflow for optimizing the input mesh for analysis would yield fewer glitches in the feedback data. Using multiple meshes could also reduce analysis faults by allowing the meshes to be checked against each other to identify and cull unreliable data. Another possibility would be to pre-record the feedback data and store it in a database for future use. This would make it possible to preview the data and cull any unreliable values beforehand, but also make the data immediately available for visualization instead of having to be recomputed after every change. This would afford an instantaneous feedback loop, providing a superlative user experience. This separation of the actual simulation from the user's experience could provide a more effective learning tool by maximizing feedback speed and reducing the range of exploration.

⁴⁴ See Appendix A

Best Time Range

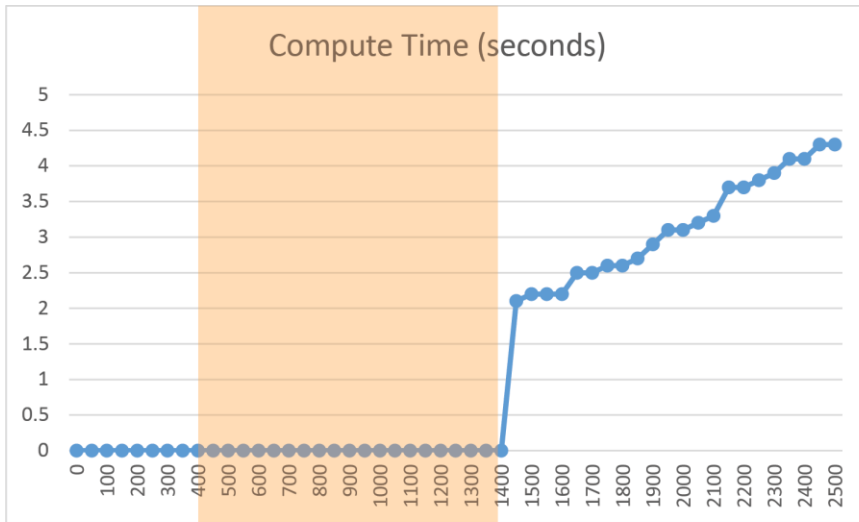
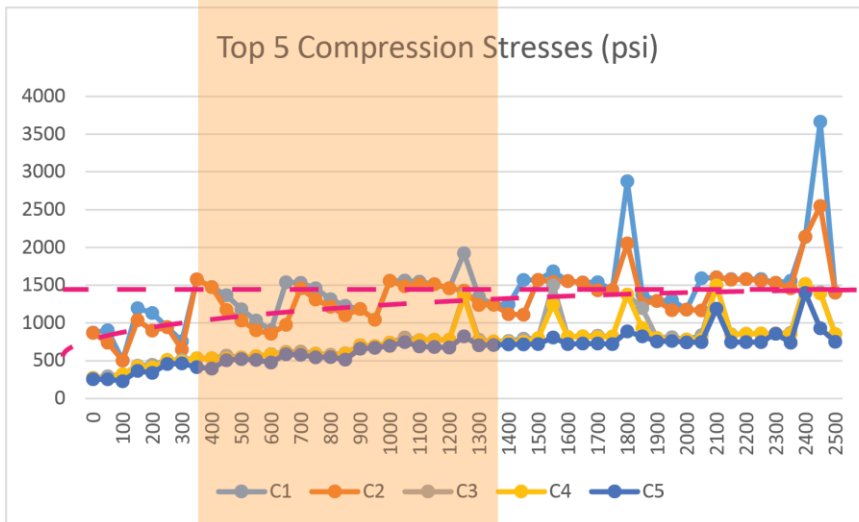
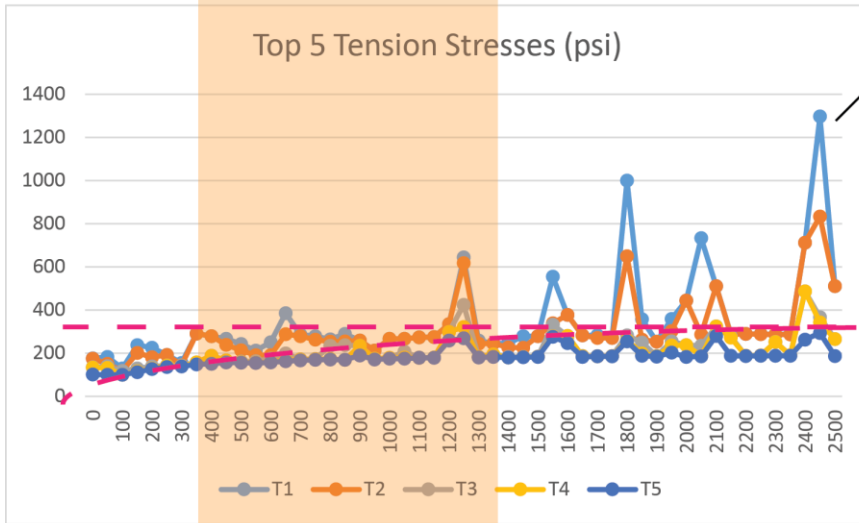


fig. 40 Analysis of the mesh sensitivity test for one form. The graphs were used to cross check appropriate compute times with stress values' presumed accuracy. The result of this particular form study was that a sensitivity value between 400 and 1200 was appropriate, a relatively wide range.



Conclusions

The acceptable standards for the mesh sensitivity and validation models are relatively low-fidelity, but that is all this tool requires. Since it is meant to be a learning tool and not a precision analysis tool, the user only needs to get an idea of how their most recent design move affected the solution's performance. The timeframe in which the user gets this information is the strength of learning tools like HyParActive.

To build experience and design knowledge, the user needs to see if their design decisions play out how they expect. Before any sort of digital performance analysis tools were available, the only way to get this information was to see the project through to completion and only then be able to judge its performance. The introduction of these tools shortened the time it took the user to get this information by offering them a very good guess of how the project would perform.

As these analysis tools become more available and easy to use, they can be implemented very early in the design process. In terms of thin shell construction, no longer does the architect need a personal mastery of geometry or to stick to symmetrical forms and rules of thumb to start with a concept that has some proof of viability. Furthermore, compacting the feedback loop to instantaneous allows the user to build intuition and "get a feel" for how the structures work.

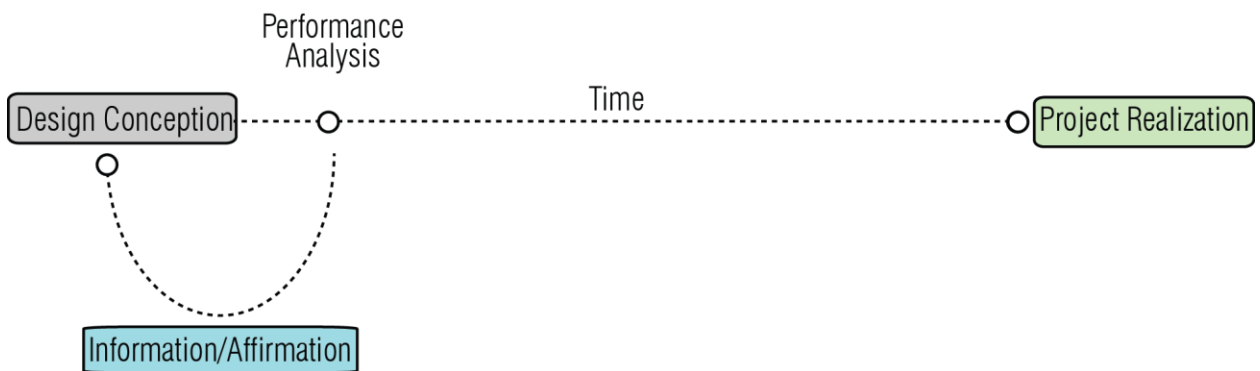
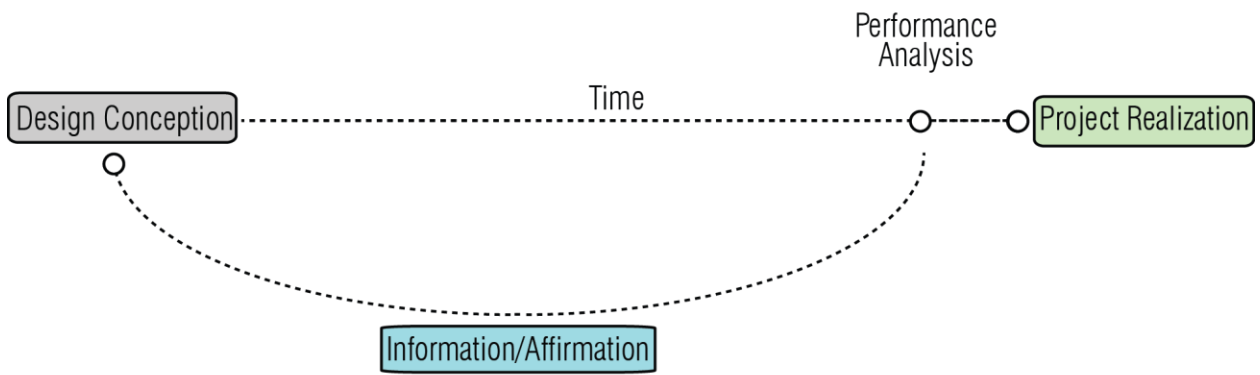
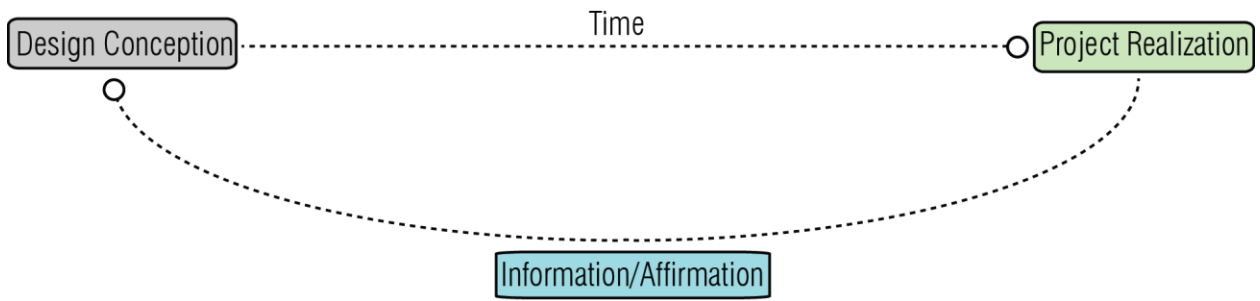


fig. 41 Diagram: The ability to utilize performance analysis earlier in the design phase lets designers make more-informed decisions and start from viable concepts

Further Opportunities

One feature that a tool like HyparActive would benefit from is a complementary fabrication workflow. Using the form output from the exploration tool, this additional workflow could generate formwork or rationalize the form into components to be fabricated and assembled. This could also be useful during the form exploration, and allow the user to explore how different materials and methods of subdivision and construction affect the performance just as the geometry does. Recent trends show that this additional workflow would be necessary to efficiently construct the complex, asymmetrical forms generated with tools like this one.

A user study would be invaluable in determining the effectiveness of the control scheme, color scheme and overall organization of the tool. Testing in a classroom setting would be the ideal benchmark for a learning tool, and some considerations have been made for a better classroom experience. Instead of giving the student a single exploration model developed for both learning and design exploration, a more efficient system may be a two-model tool. This tool would focus on learning with less freedom and more instruction in the first model to assure the principles are understood, and then in the second step give much more freedom for exploration. This additional tutorial model would give the user a high level of control over one abstract hyper form to focus on geometry and stresses before needing to worry about space and physical constraints. Limiting the control scheme in this stage would make instruction in a classroom setting much easier and would help make sure core concepts were covered.

As analysis tools develop and become easier to use, their effect on the computational design process grows more profound. Their inclusion earlier in the process and ability to provide increasingly accurate results makes them valuable to the designer and student. By compacting the design feedback loop, not only is the user afforded the ability to develop sound concepts without the need for extensive expertise, but also the ability to gain this expertise. It is hoped that more learning tools are developed that make it easier for complex forms and metrics to be explored and that afford designers an increasing number of efficient solutions to investigate.

Bibliography

- Bechthold, Martin. *On Shells and Blobs*. *Scientific Electronic Library Online*. CONICYT-Chile. Web.
- Burger, N., and D. P. Billington. "Felix Candela, Elegance and Endurance: An Examination of the Xochimilco Shell." *IASS Journal* 47.3 (2006): 271-78. IASS. Web.
- Garlock, Maria E., David P. Billington, and Noah Burger. *Félix Candela : engineer, builder, structural artist*. New Haven, Conn. London: Yale University Press, 2008. Print.
- Isler, Heinz. "Concrete Shells Derived from Experimental Shapes." *Structural Engineering International* 4.3 (1994): 142-47. Ingenta Connect. Web.
- Kaczynski, M., W. McGee, and D. Pigram. "Robotically Fabricated Thin-shell Vaulting." *Proc. of Association for Computer Aided Design in Architecture*. 2011. Web. 14 Nov. 2014.
- Krivoshapko, S. N., Christian A. Bock Hyeng, and I. A. Mamieva. "Chronology of Erection of the Earliest Reinforced Concrete Shells." *International Journal of Research and Reviews in Applied Sciences* 18.2 (2014): 95-108. IJRRAS. Web. 16 Feb. 2016.
- Kuma, T. "Shrink Film Architecture." Association of Computer Aided Architectural Design in Asia. 2014. 22 Apr. 2014. Web. 14 Nov. 2014.
- Kuma, T., M. Dorstelmann, M. Prado, and A. Menges. "Integrative Computational Design Methodology for Composite Spacer Fabric Architecture." *Proc. of Education and Research in Computer Aided Architectural Design in Europe*. 2014. Web. 14 Nov. 2014.
- Lozano-Galant, Jose Antonio, and Ignacio Payá-Zaforteza. "Structural Analysis of Eduardo Torroja's Frontón De Recoletos' Roof." *Engineering Structures* 33.3 (2011): 843-54. ScienceDirect. Web.
- Martins, Pedro Filipe, Paulo Fonseca De Campos, Sandra Nunes, and Jose Pedro Sousa. "Prefabrication in Concrete Through Robotic Hot-Wire Cutting." *ECAADe* 33 2 (2015): 341-51. CUMINCAD. Web.
- Melaragno, Michele G. *An Introduction to Shell Structures: The Art and Science of Vaulting*. New York, NY: Van Nostrand Reinhold, 1991. Print.
- Meyer, Christian, and Michael H. Sheer. "Do Concrete Shells Deserve Another Look?" *Concrete International* 27.10 (2005): 43-50. EBSCO Host. Web.
- Peerdeman, Bart, J. C. Walraven, W. J. M. Peperkamp, J. G. Rots, P. C. J. Hoogenboom, and I. J. M. Houben. "Analysis of Thin Concrete Shells Revisited: Opportunities Due to Innovations in Materials and Analysis Methods." Thesis. Delft University of Technology, 2008. Tufdelft.nl. Delft University of Technology. Web.
- Rael, Ronald, and Virginia San Fratello. "Developing Concrete Polymer Building Components for 3D Printing." *ACADIA 2011* (2011): 152-57. CUMINCAD. Web.
- Raspall, Felix, Matias Imbern, and William Choi. "Adaptive Tectonic Systems: Parametric Modeling and Digital Fabrication of Precast Roofing Assemblies Toward Site-Specific Design Response." *CUMINCAD. Proc. of ACADIA 13, Cambridge*. Web.
- Reichert, S., T. Schwinn, R. Magna, F. Waimer, J. Knippers, and A. Menges. "Fibrous Structures." *Computer-Aided Design* 2014: 27-39. Web. 14 Oct. 2014.
- Schipper, H. R., and S. Grünwald. "Efficient Material Use Through Smart Flexible Formwork Method." *Proc. of ECO-Crete: International Symposium on Environmentally Friendly Concrete, Reykjavik, Iceland*. Tufdelft.nl. Web.
- Schwinn, Tobias, Oliver David Krieg, and Achim Menges. "Behavioral Strategies: Synthesizing Design Computation Adn RObotic Fabrication of Lightweight Timber Plate Structures." *ACADIA 2014* (2014). Research Gate. Web.

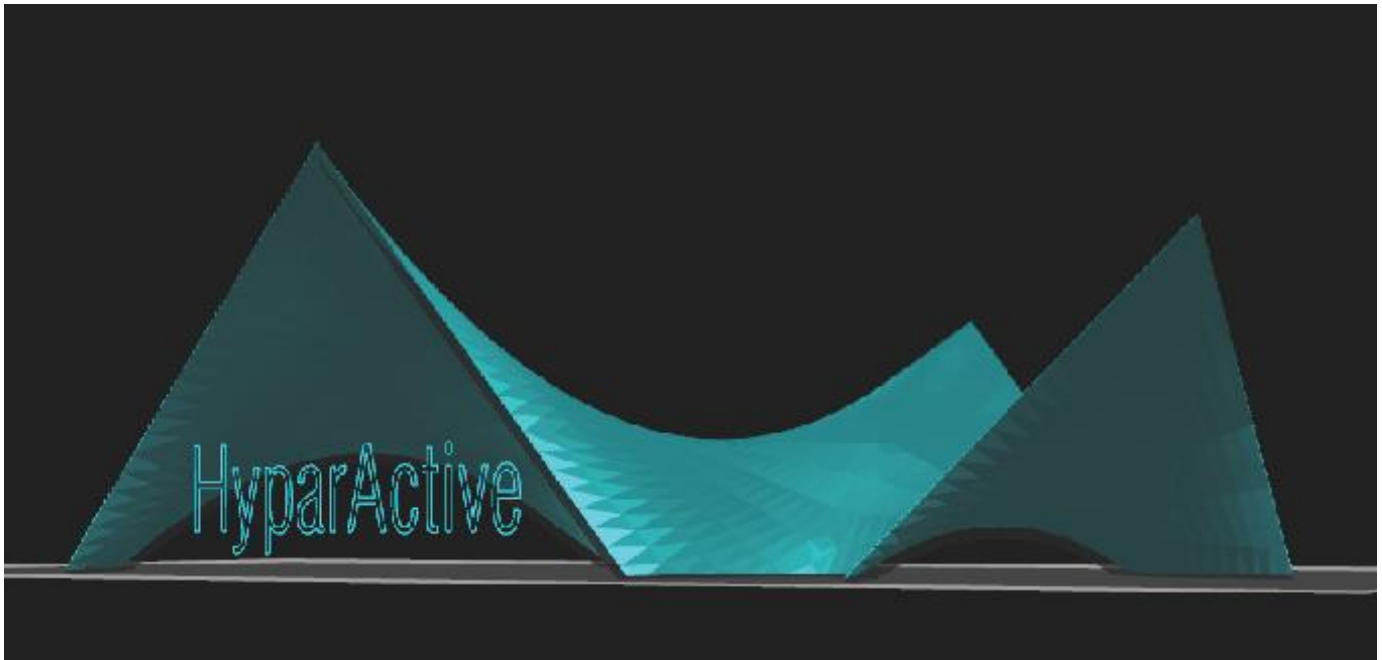
Veenendaal, Diederik, and Philippe Block. "Design Process for Prototype Concrete Shells Using a Hybrid Cable-net and Fabric Formwork." *Engineering Structures* 75 (2014): 39-50. ScienceDirect. Web.

Weller, Mike. "Form Finding, Force and Function: Mass-Spring Simulation for a Thin Shell Concrete Trolley Barn." Thesis. University of Washington, 2011. Design Machine Group Publications. Web.

Figure Sources

- Fig. 1 <http://tectonicablog.com/wp-content/uploads/2012/04/Marie-Eug%C3%A8ne-Freyssinet-4.jpg>
- Fig. 2 <https://s-media-cache-ak0.pinimg.com/564x/45/1e/54/451e54aca70f8e213283b425c03306bc.jpg>
- Fig. 3 <https://travelpast50.com/wp-content/uploads/2014/07/centennial-hall-wroclaw.jpg>
- Fig. 4 http://www.do-it-at-leipzig.de/csdata/image/1/de/venue_kohlrabizirkus_leipzig_the_market_hall_around_1933...
- Fig. 5 <http://explorepahistory.com/displayimage.php?imgId=1-2-1442>
- Fig. 6 <http://theredlist.com/wiki-2-19-879-605-224910-view-nervi-pier-luigi-profile-nervi-pier-luigi-palazzetto-dello-sp...>
- Fig. 7 http://www.enriquecarrazoni.com/index2.php_files/Felix%20Candela_02.jpg
- Fig. 8 ecommons.cornell.edu
- Fig. 9 from author
- Fig. 10 <http://cdn.archinect.net/images/514x/k8/k86en218k808wn6h.jpg>
- Fig. 11 <http://blog.buildllc.com/wp-content/uploads/2009/04/heinz-isler-deitingen-01.jpg>
- Fig. 12 <https://s-media-cache-ak0.pinimg.com/736x/d6/79/6d/d6796d213959d092a2ee8455f9532848.jpg>
- Fig. 13 <https://wewanttorearn.files.wordpress.com/2011/11/munich-stadium-10.jpg?w=1200&h=>
- Fig. 14 <http://www.armstrongsteelbuildings.com/steel-building-prices/images/01.jpg>
- Fig. 15 <http://deathofdrawing.com/wp-content/gallery/chapter-5/FEA-max-principal-stress-psi.jpg>
- Fig. 16 from author
- Fig. 17 https://static.dezeen.com/uploads/2010/05/dzn_Fatty-Shell-2.jpg
- Fig. 18 http://matsysdesign.com/wp-content/uploads/2013/09/IMG_8866_clean_1200-620x413.jpg
- Fig. 19 http://lbn.sika.com/content/near_east/main/en/concrete-redirect/sika-concrete-technology/concrete-handbook...
- Fig. 20 <http://i.imgur.com/OeuS7Fu.png>
- Fig. 21 <http://i.imgur.com/hUBlxBs.png>
- Fig. 22 from author
- Fig. 23 <http://www.designboom.com/wp-content/uploads/2013/03/robotpav01.jpg>
- Fig. 24 http://ad009cdnb.archdaily.net/wp-content/uploads/2013/03/5136aa04b3fc4b828e000238_icd-itke-resea...
- Fig. 25 http://www.achimmenges.net/wp-content/gallery/landesgartenschau_icd-itke/stuttgart_02.JPG
- Fig. 26 – 47 from author

Appendix A: HyparActive User Manual



HyparActive User Manual

HyparActive is a design exploration tool that generates and analyzes a hyperbolic paraboloid shell. This tool is the product of research that explores utilizing parametric modeling in conjunction with lightweight performance analysis tools to help designers learn about unfamiliar geometries and structural systems.

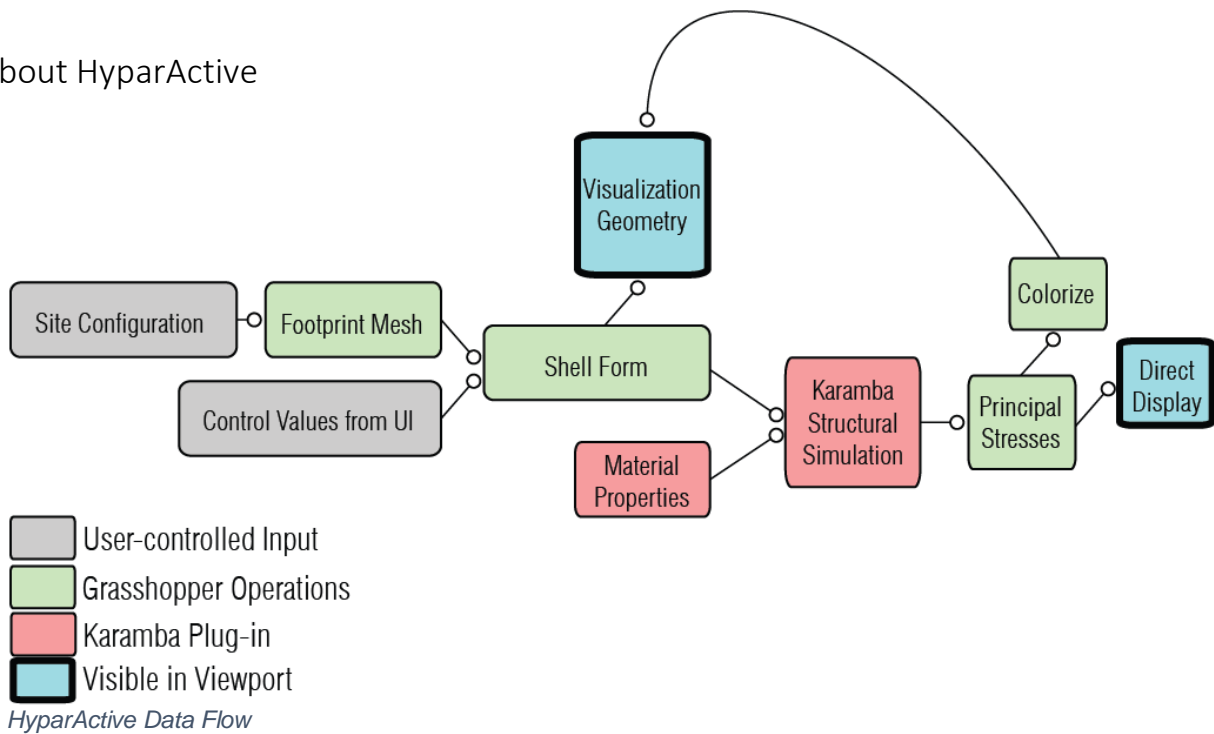
This tool was developed as part of Winston Davis' MS.dc thesis and is available for download as a Grasshopper file at:
dmg.be.washington.edu/projects/hyparactive

Getting Started

There are some prerequisites to using the tool. You will need to have installed:

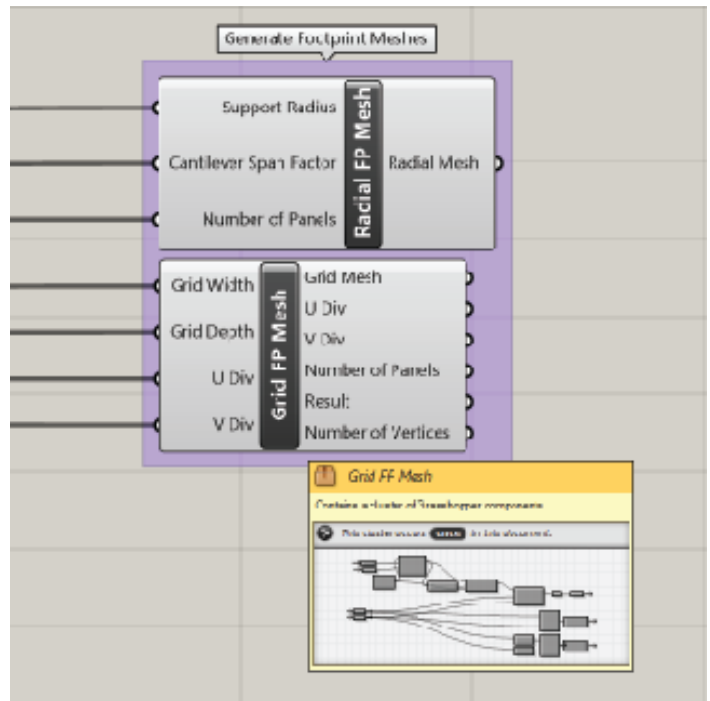
Rhino 3D- www.rhino3d.com/download.htm
Grasshopper - www.grasshopper3d.com
Karamba - www.karamba3d.com
Human UI - www.food4rhino.com/project/human-ui

About HyparActive



Tool Organization

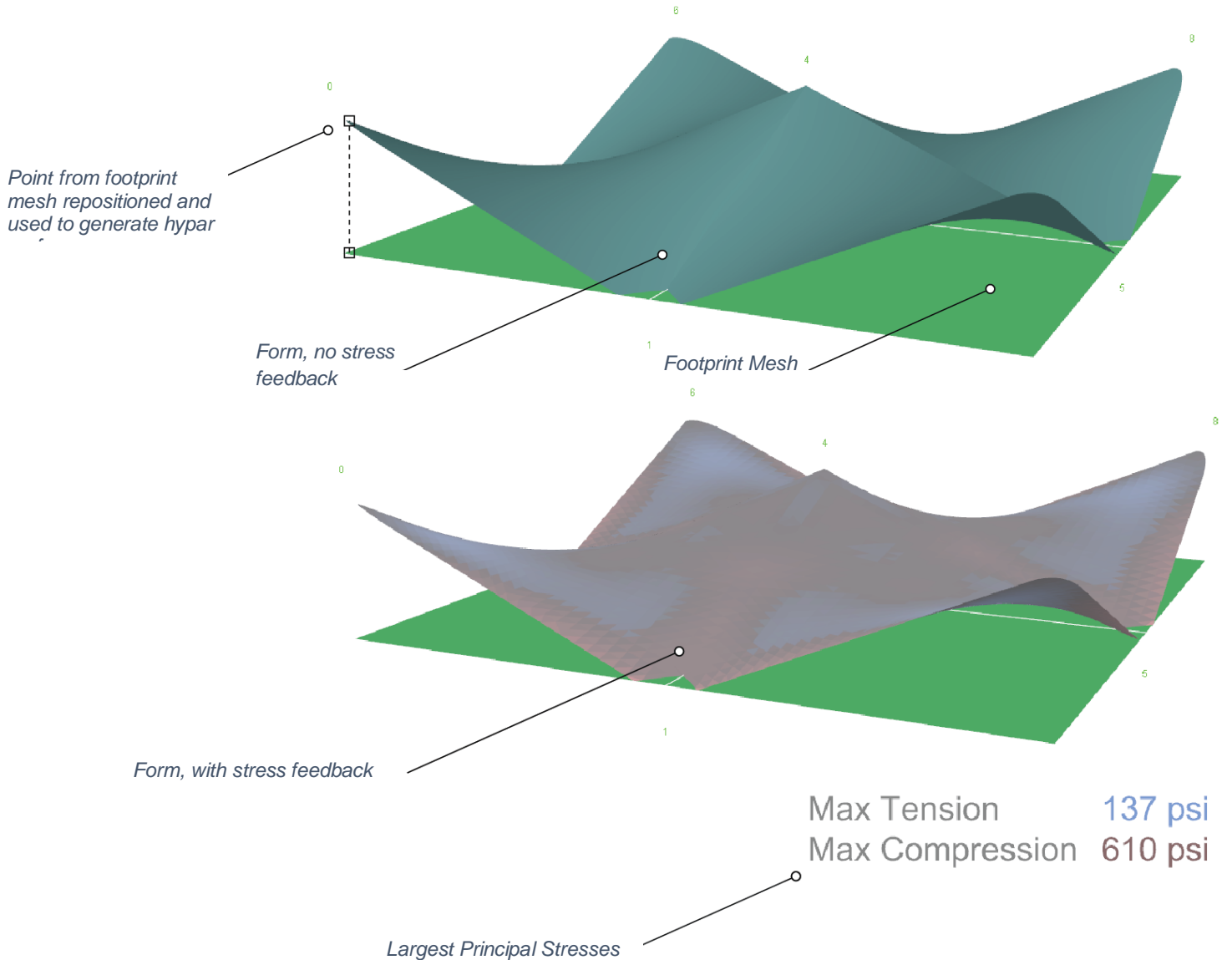
The Grasshopper definition is organized so that the user can dive deeper into in aspect of the tool as they become comfortable. Using the "cluster" option in Grasshopper, top-level clusters represent high-level aspects of the tool, and contain components and clusters that continually get more specific.



Compartmentalization of the definition using "clusters"

In the Viewport

In the Rhino viewport, the user will be able to see the footprint mesh and the shell form with various visualization options. The form parameters and visualization options are controlled in a separate window (see next page). When the structural simulation is activated, the form is colored based on the stresses in each element/mesh face.



UI Organization

The workflow and UI is organized into three main sections: Site, Form and Analyze. In the Site tab, the user configures the footprint mesh.

Site

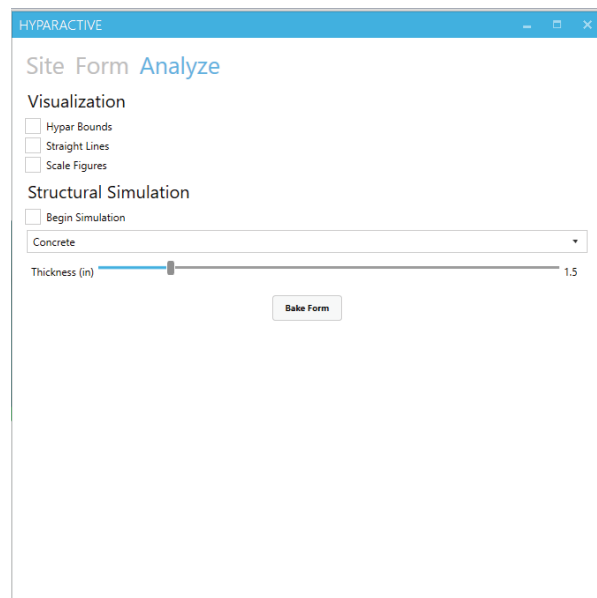
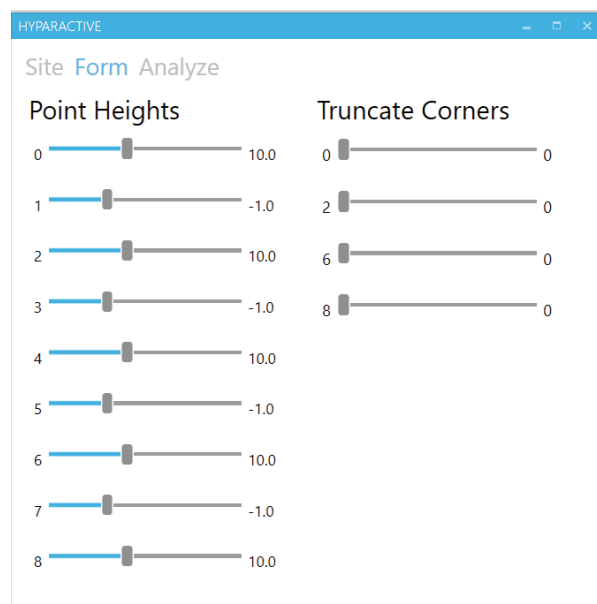
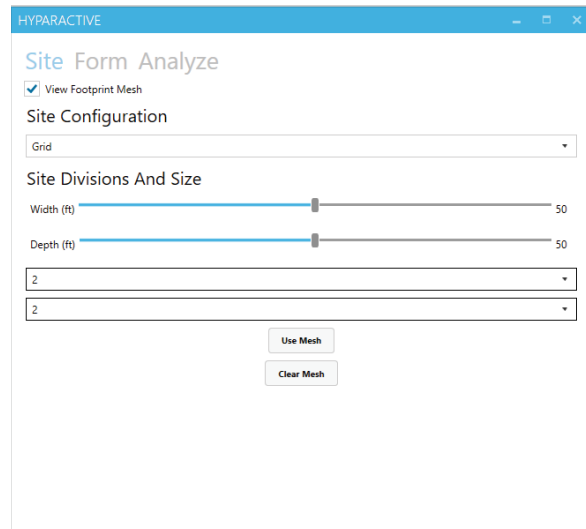
1. Choose to view the footprint mesh
2. Choose configuration of footprint
3. Specify dimensions and number of segments
4. Use the current footprint configuration
5. Clear the current footprint configuration

Form

6. Adjust heights of each point in the footprint mesh to alter the form
7. Truncate the corner hyper surfaces for rounder edges

Analyze

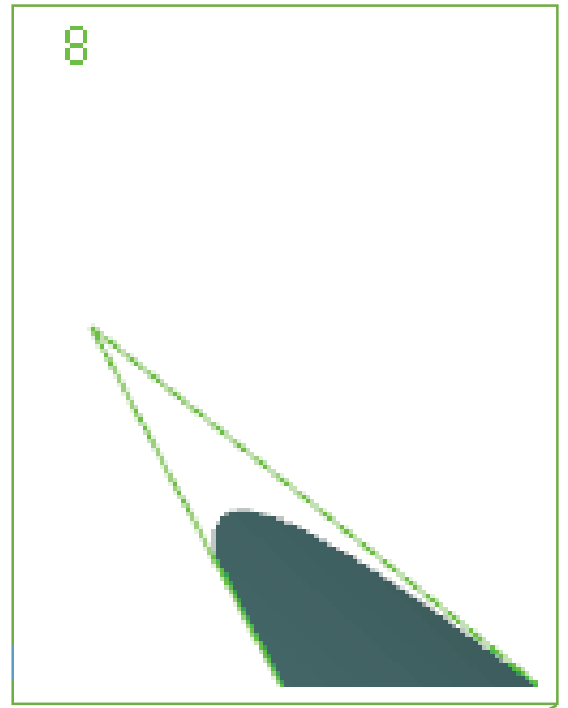
8. Toggle geometric and scale figure visualizations
9. Turn on structural simulation
10. Material picker (Under Construction)
11. Shell thickness
12. Save (Bake) form to Rhino model



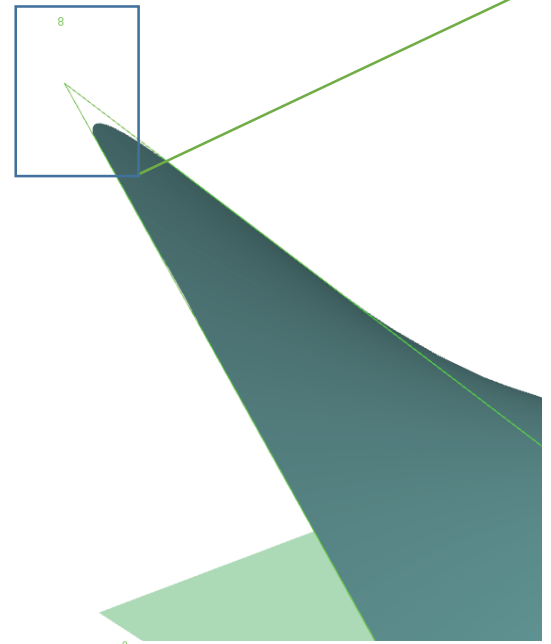
Points to Surface

Each point from the footprint mesh is repositioned at a new height and used to generate the hyper form. To know which slider controls which point, an index number at each point matches the label of the controlling slider.

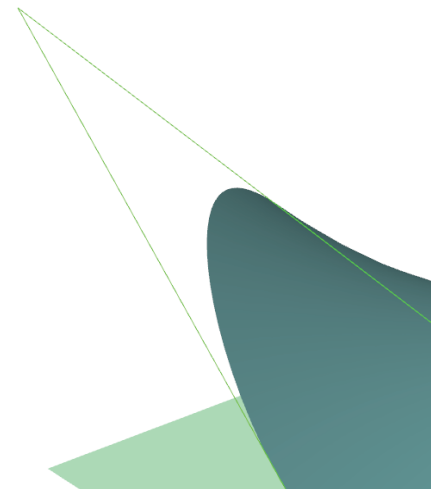
Some corners of the form can be truncated with sliders in a separate group. The same index value will denote this slider, if available. Truncating the corner will not affect the position of the controlling point, so the two parameters will need to be used jointly to control the height of the form's edge.



Un-truncated hyper corner



Truncated hyper corner

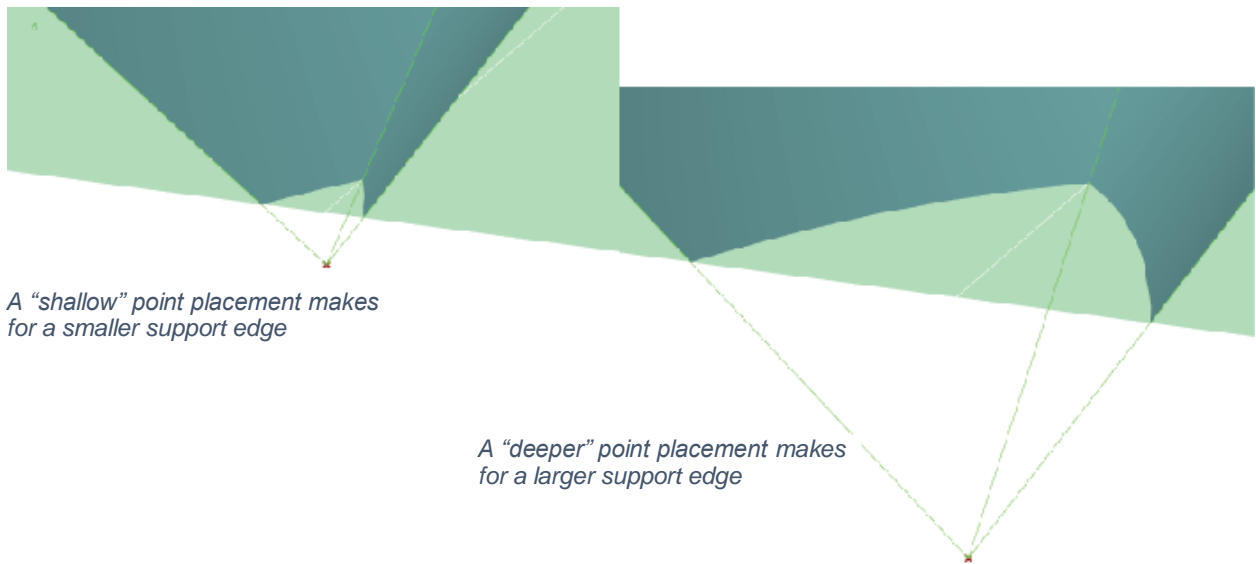
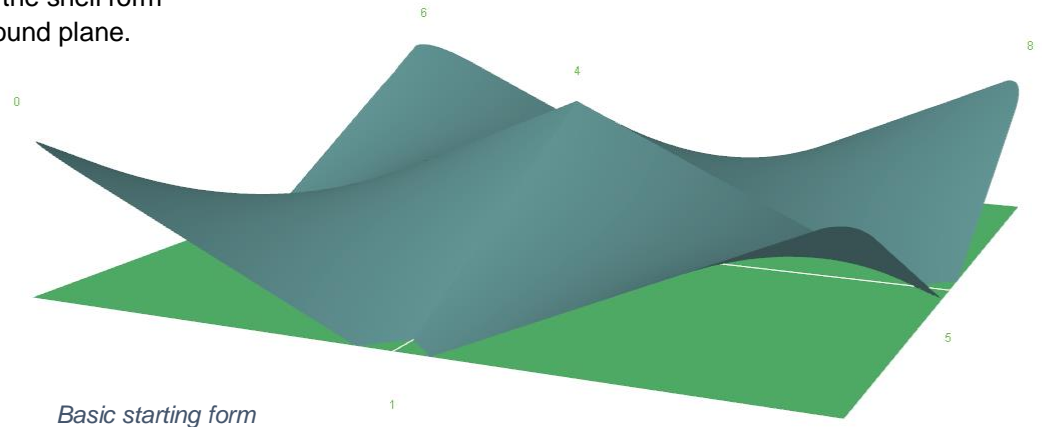


Surface to Shell

When “Use Mesh” is clicked, a basic form is generated to start from. This initial form suggests which points to keep below zero for best results. These points below the ground plane control the amount of shell material in contact with the ground.

Currently, at least one point must be below zero for a form to be generated.

To increase support at a particular location, pull the mesh point further below zero to increase the width of the shell form intersected by the ground plane.

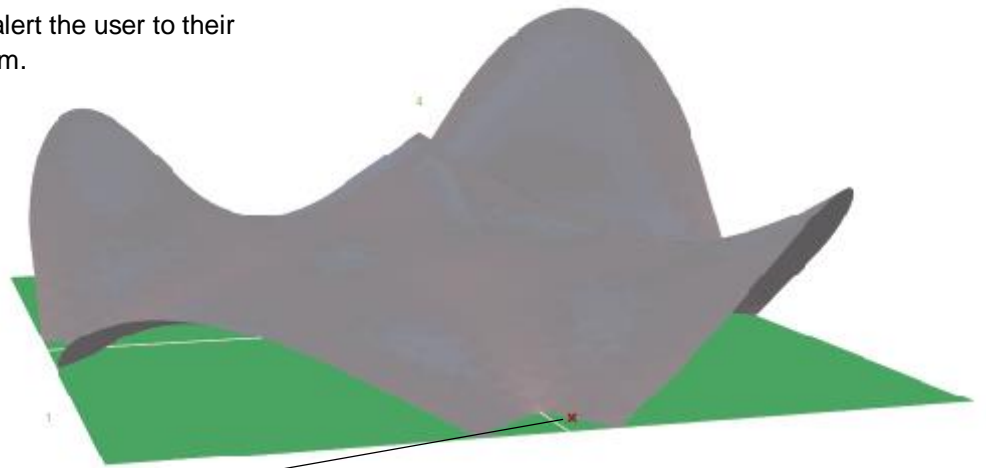


Problem Elements

The occurrence of relatively-miniscule elements in the analysis mesh is possible and unpredictable. These problem elements produce highly-inaccurate stress values that degrade the fidelity of the analysis. A system for generating a more uniformly-subdivided mesh is being developed; meanwhile, a simple solution to these problem elements provides a quick fix.

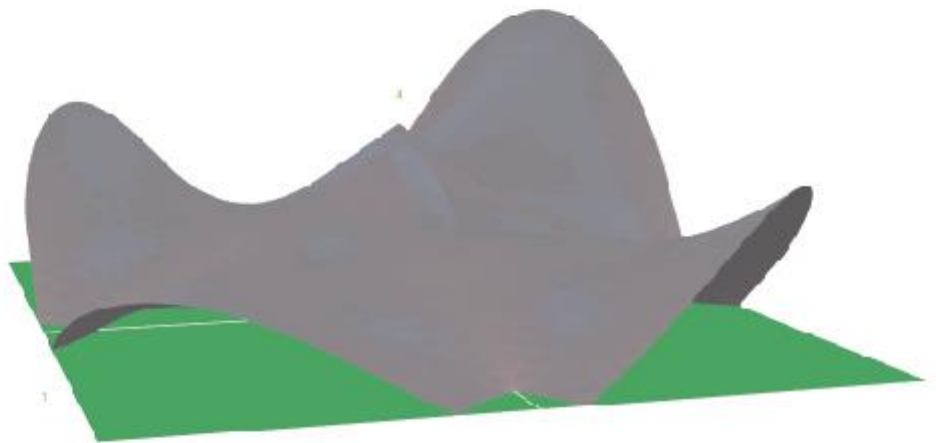
While the bogus stress values are usually easy to identify, these elements' sham values will be culled from what is displayed on screen. The elements themselves will be tagged in the 3D model view to alert the user to their presence and position on the form.

Making slight, localized adjustments to the form near the problem element has been observed to consistently resolve the problem by generating a more uniformly-subdivided mesh.



Location of problem element

Max Compression	2713.0 psi
Max Tension	465.0 psi



Moving the nearest support point 2 feet resolved the problem element and caused unnoticeable changes to the form

Max Compression	500.0 psi
Max Tension	90.0 psi

Interpreting the Feedback

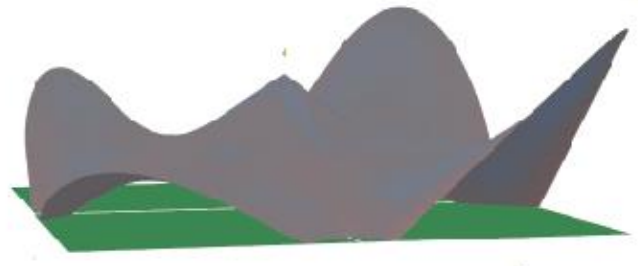
The coloration of the mesh is controlled by the stresses present in each individual element/mesh face. The larger principle stress in each face, either in tension or compression, is used to determine the color gradient used to color that mesh.

If both stresses are negligible, the face is colored gray.

If the tensile stress is larger, the face becomes brighter blue the larger it is. The same goes for compression, but in red.

If a stress goes over the threshold for the material, the face is colored in black to signify that the structure would fail there.

Low stresses resulting in dull coloration



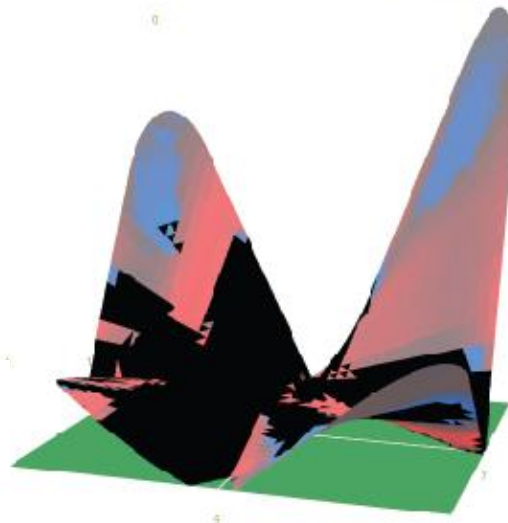
Max Compression	342.0 psi
Max Tension	217.0 psi

High stresses, resulting in brighter coloration



Max Compression	1624.0 psi
Max Tension	503.0 psi

Stresses over the material threshold results in black coloration to denote structural failure



Max Compression	239536.0 psi
Max Tension	63371.0 psi

Appendix B: Mesh Sensitivity Test Results

Tested Forms

Three different forms were used to find an appropriate sensitivity value. The forms were analyzed using a range of sensitivity values starting at 0 and increasing by 50. The five highest values of each principal stress were recorded to identify an asymptotic curve that would provide a benchmark value to gauge the accuracy of the individual sensitivity settings. The time it took to calculate the solution was also measured for each iteration to help identify the most useful range.

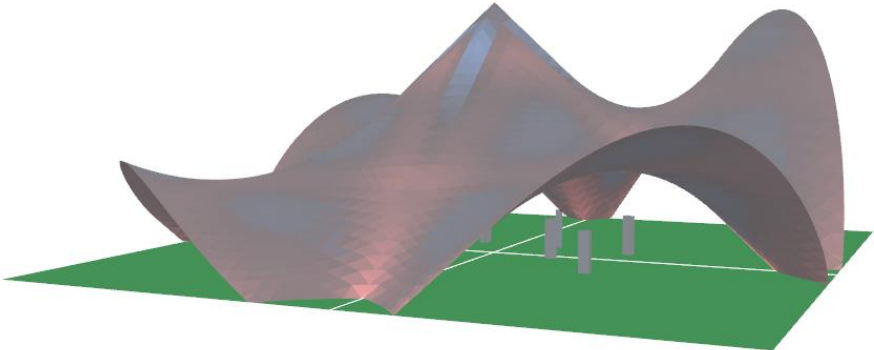


fig. 42 Test form 1

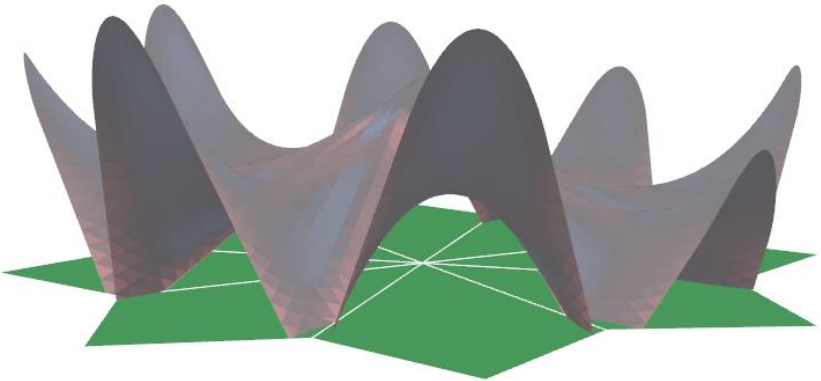


fig. 43 Test form 2

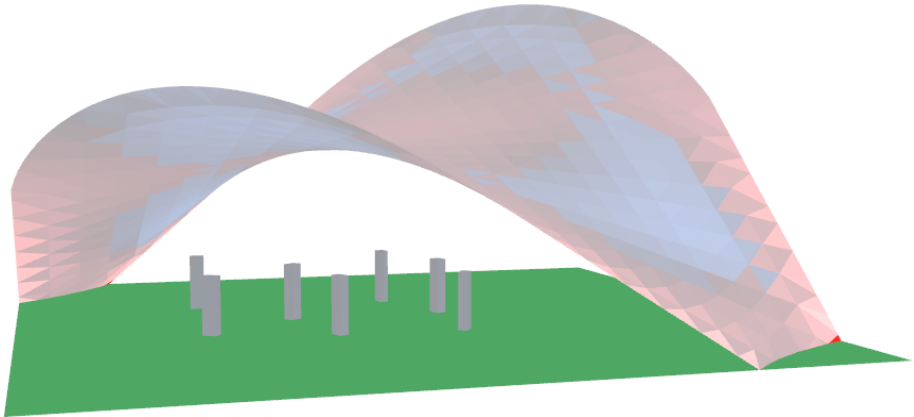


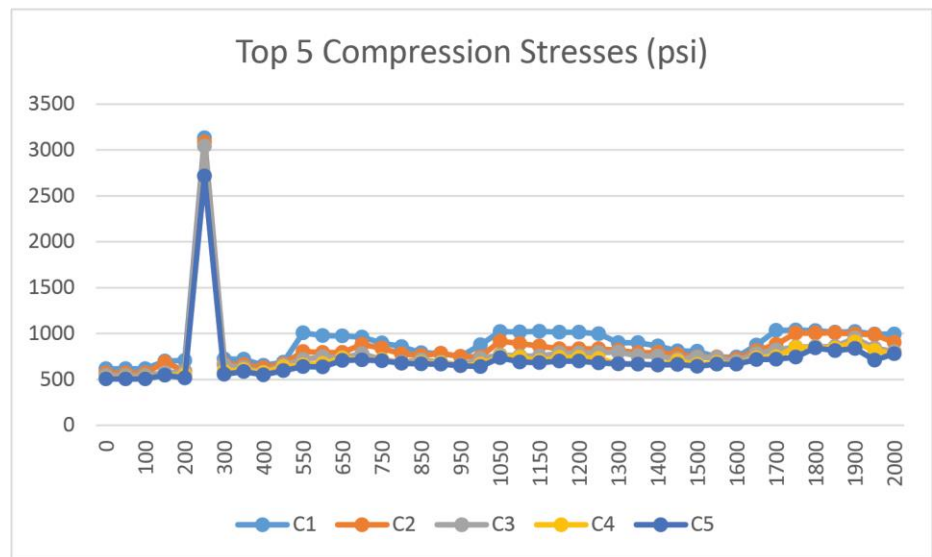
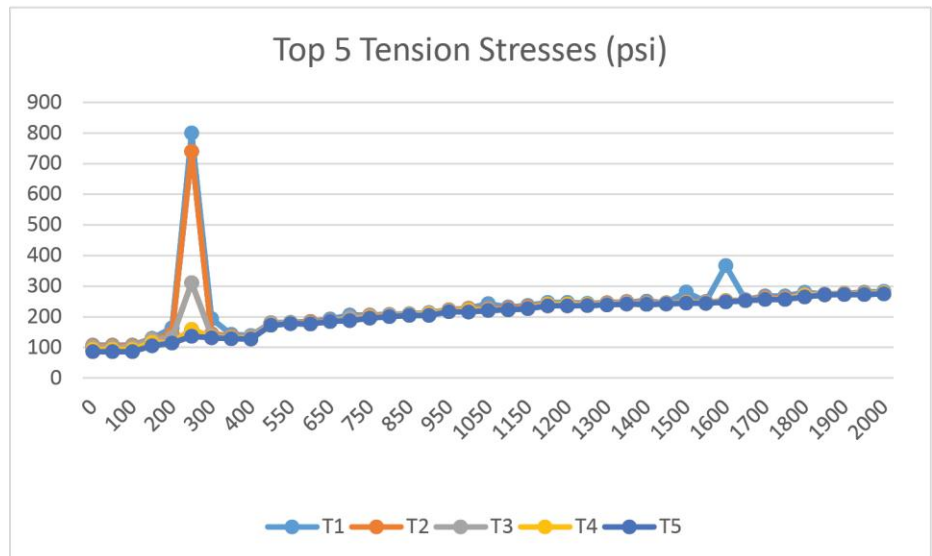
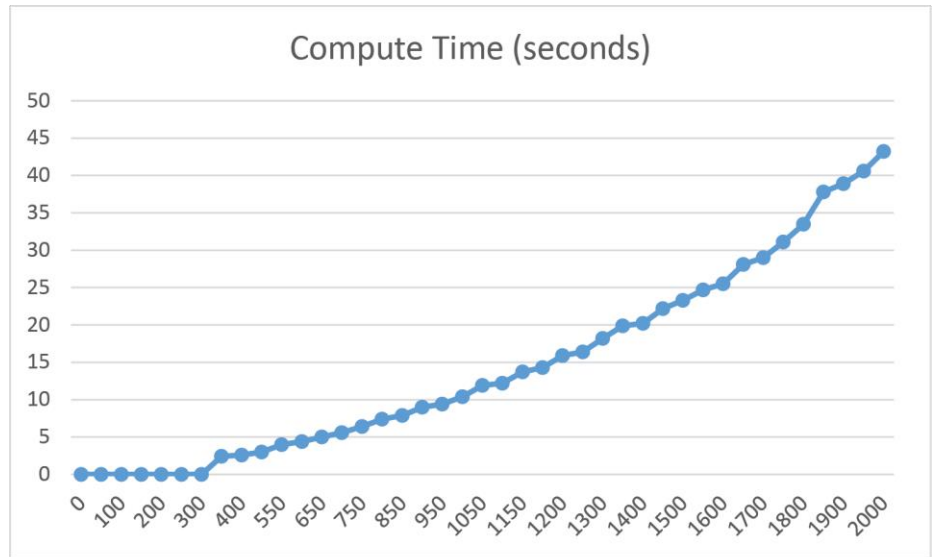
fig. 44 Test form 3

Form 1 Data

Sens.	E	Five Largest Tension Stresses					Five Largest Compression Stresses					Sec.
		T1	T2	T3	T4	T5	C1	C2	C3	C4	C5	
0	841	107	105	101	93	86	615	570	543	513	506	
50	841	107	105	101	93	86	615	570	543	513	506	0
100	841	107	105	101	93	86	615	570	543	513	506	0
150	1283	129	126	125	116	105	700	688	572	547	546	0
200	1647	163	145	132	115	114	706	593	583	548	517	0
250	1941	800	740	311	158	136	3132	3085	3041	2716	2716	0
300	2262	194	144	138	134	131	723	668	655	590	557	0
350	2619	142	136	133	130	128	719	661	630	605	586	2.4
400	2876	138	135	134	129	127	654	627	580	574	548	2.6
500	3784	181	180	178	173	172	686	669	655	636	597	3
550	4091	182	180	179	178	177	1006	804	716	658	640	4
600	4420	185	184	180	176	176	976	793	746	674	637	4.4
650	4737	193	187	186	185	185	975	794	735	734	707	5
700	5111	206	198	197	189	188	962	879	779	716	714	5.6
750	5479	206	205	202	199	196	897	839	718	717	703	6.4
800	5850	208	207	206	202	201	857	778	686	677	676	7.4
850	6245	210	208	208	207	205	789	761	712	683	671	7.9
900	6448	214	212	212	210	205	785	782	686	679	667	9
950	6855	223	222	220	219	217	751	750	655	649	648	9.4
1000	7278	228	227	224	222	216	877	748	727	665	640	10.4
1050	7491	243	228	225	222	221	1021	917	767	751	736	11.9
1100	7918	232	228	224	223	223	1019	890	756	741	691	12.2
1150	8129	237	233	229	228	227	1023	865	753	702	683	13.7
1200	8592	247	242	242	241	236	1013	834	787	741	699	14.3
1200	8592	247	242	242	241	236	1013	834	787	741	699	15.9
1250	8818	244	241	240	240	237	997	832	793	725	681	16.4
1300	9284	246	245	243	240	239	902	817	798	671	670	18.2
1350	9551	250	249	247	243	242	901	789	755	670	667	19.9
1400	9788	251	246	243	241	241	863	793	752	656	656	20.2
1450	10287	246	245	244	243	242	810	769	724	704	663	22.2
1500	10565	281	249	248	247	245	808	747	740	664	642	23.3
1550	10820	250	248	247	245	244	744	742	735	684	665	24.7
1600	11078	367	253	252	251	249	744	723	695	671	667	25.5
1650	11607	256	255	255	253	253	873	815	783	736	716	28.1
1700	11863	268	263	259	258	257	1034	882	819	745	719	29
1750	12194	268	262	259	258	257	1037	1003	855	847	743	31.1
1800	12602	280	274	274	270	265	1032	1005	857	849	845	33.5

Data Table: The values in the table were recorded at each sensitivity value (Sens.). The other recorded values were the number of elements (E), the five largest tension stresses (T1-T5) and compression stresses (C1- C5), and the time in seconds it took to compute the solution (Sec.)

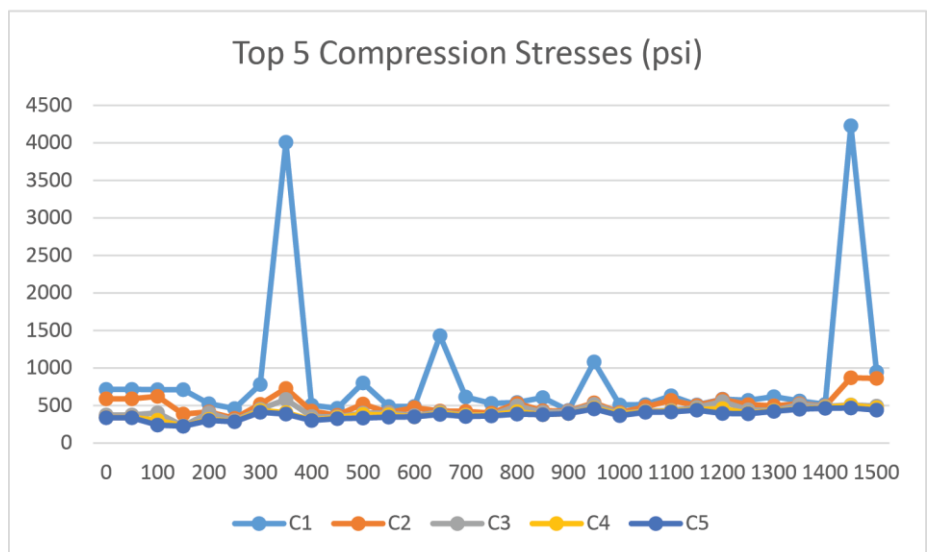
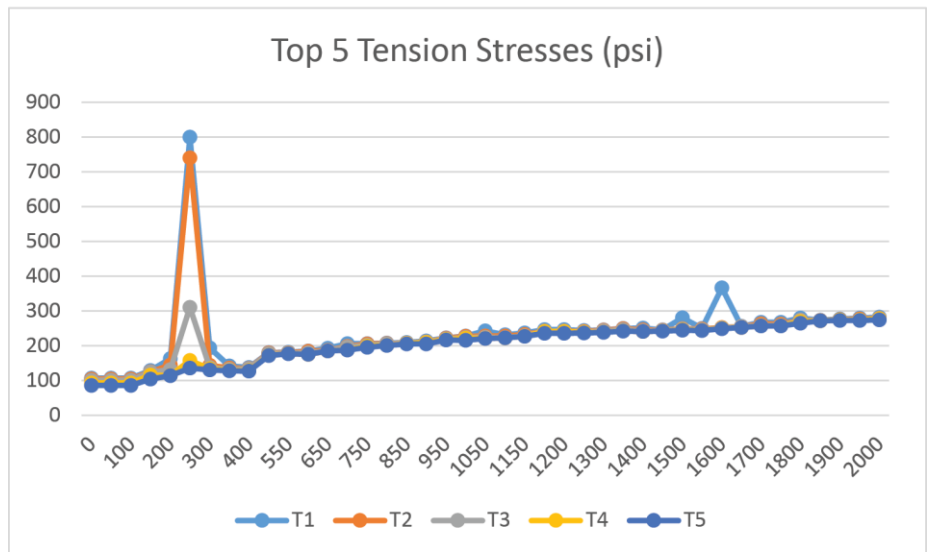
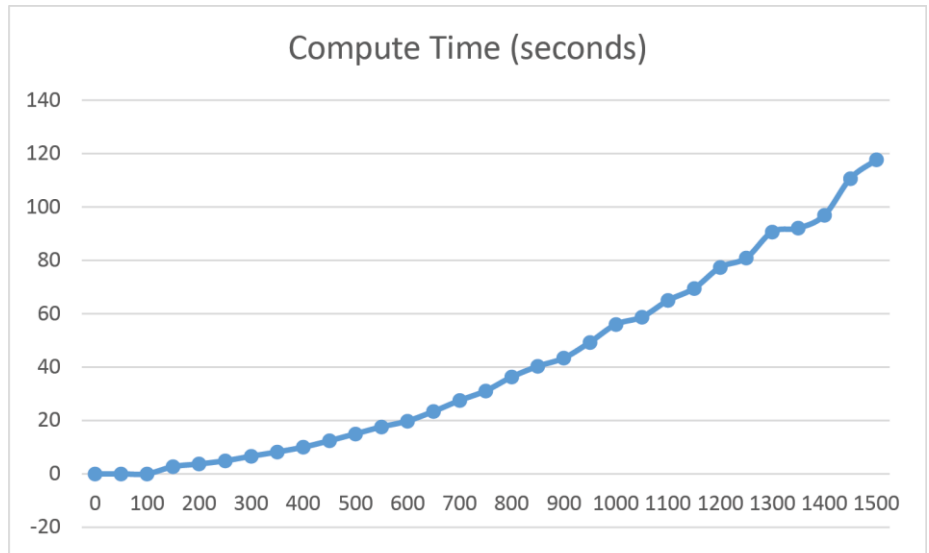
fig. 45 Graphical Form 1 Data



Form 2 Data

Sens.	E	Five Largest Tension Stresses					Five Largest Compression Stresses					Sec.
		T1	T2	T3	T4	T5	C1	C2	C3	C4	C5	
0	1624	122	117	116	80	58	715	592	375	343	339	0
50	1624	122	117	116	80	58	715	592	375	343	339	0
100	1877	137	101	92	71	68	712	623	403	306	240	0
150	2718	137	94	88	86	85	714	387	230	228	225	2.7
200	3528	97	95	89	87	87	525	418	404	318	301	3.7
250	4210	113	109	103	100	98	462	330	302	290	285	4.9
300	4958	1029	158	122	114	114	782	519	451	436	413	6.6
350	5783	20324	579	461	151	124	4008	730	584	407	387	8.2
400	6390	130	124	119	118	113	507	429	355	312	304	10
450	7269	1064	1018	872	641	460	463	371	350	344	326	12.4
500	7934	4494	1110	863	443	399	801	521	401	383	335	15
550	8619	1178	142	130	128	127	490	409	406	379	348	17.6
600	9322	146	135	132	129	124	490	472	369	353	352	19.8
650	10075	7657	182	178	167	146	1431	429	418	401	384	23.4
700	10839	777	594	140	138	135	617	423	376	372	357	27.5
750	11644	749	592	142	136	134	529	398	377	376	362	31.1
800	12487	932	726	333	281	162	542	531	496	421	386	36.3
850	13337	1234	393	294	144	141	609	433	414	380	378	40.3
900	13833	1308	145	141	139	138	437	429	419	395	394	43.4
950	14696	6013	1480	1386	1120	783	1084	537	516	469	455	49.3
1000	15610	338	294	151	141	141	510	407	396	387	369	56
1050	16088	151	144	143	143	142	514	484	429	419	412	58.8
1100	17079	3763	3511	1160	905	630	633	572	438	428	415	65
1150	17589	2045	1307	1018	426	348	510	500	478	448	441	69.5
1200	18599	148	145	145	142	140	585	581	555	459	396	77.4
1250	19124	1206	319	254	155	149	570	513	446	401	390	80.9
1300	20193	1559	1239	851	840	667	618	496	438	436	425	90.7
1350	20738	150	150	149	143	142	564	525	512	457	451	92.1
1400	21303	1354	1044	695	553	479	516	495	490	476	463	96.9
1450	22418	21803	4895	2909	553	404	4229	871	508	506	468	110.7
1500	22980	5508	4841	2954	526	414	950	862	493	474	442	117.7

fig. 46 Graphical Form 2 Data



Form 3 Data

Sens.	E	Five Largest Tension Stresses					Five Largest Compression Stresses					Sec.
		T1	T2	T3	T4	T5	C1	C2	C3	C4	C5	
0	117	176	175	134	133	101	870	868	275	268	254	0
50	129	182	151	140	132	99	901	738	292	258	253	0
100	194	129	117	117	100	100	501	501	320	320	229	0
150	288	237	201	129	116	112	1197	1036	435	421	366	0
200	378	225	181	139	129	127	1132	900	445	411	338	0
250	456	192	192	143	143	136	944	944	508	508	455	0
300	536	155	144	142	140	139	756	647	508	492	465	0
350	630	290	290	157	157	148	1575	1575	532	532	414	0
400	700	278	278	188	188	151	1472	1472	534	534	395	0
450	817	266	239	167	166	157	1367	1172	565	528	505	0
500	887	243	213	161	159	156	1179	1032	544	539	521	0
550	961	212	190	163	156	155	1031	902	559	558	510	0
600	1041	250	191	175	160	157	902	857	586	577	475	0
650	1119	385	288	199	168	162	1540	975	618	606	585	0
700	1201	286	279	172	171	167	1532	1458	619	591	579	0
750	1293	278	263	173	172	169	1457	1309	594	588	544	0
800	1377	264	253	235	173	171	1312	1213	578	559	548	0
850	1475	289	254	237	169	169	1227	1099	598	592	514	0
900	1544	258	258	235	235	189	1183	1183	703	703	657	0
950	1630	212	212	174	174	170	1042	1042	692	692	671	0
1000	1734	266	266	179	179	174	1558	1558	740	740	697	0
1050	1790	267	267	207	180	175	1561	1486	806	752	746	0
1100	1889	273	273	180	179	178	1545	1511	771	769	688	0
1150	1944	274	274	180	180	178	1512	1512	776	776	682	0
1200	2072	334	334	298	298	259	1457	1457	775	775	673	0
1250	2121	644	617	424	321	269	1922	1428	1380	1343	822	0
1300	2229	258	244	182	182	180	1346	1239	778	747	704	0
1350	2300	245	245	194	194	182	1242	1242	754	754	709	0
1400	2354	245	227	182	180	180	1245	1117	760	741	714	0
1450	2481	278	225	183	182	181	1568	1109	791	750	717	2.1
1500	2570	279	279	184	184	182	1569	1569	796	796	720	2.2

Fig. 47 Graphical Form 3 Data

